

ROBUST, CO-DESIGN EXPLORATION OF MULTILEVEL PRODUCT, MATERIAL, AND MANUFACTURING PROCESS SYSTEMS

Mathew Baby ^a, Rashmi Rama Sushil ^b, Palaniappan Ramu ^b, Janet K. Allen ^c, Farrokh Mistree ^c, Anand Balu Nellippallil ^{a,1}

^a The Systems Realization Laboratory @ FIT, Department of Mechanical and Civil Engineering, Florida Institute of Technology, Melbourne, FL 32901, USA

^b ADOPT Laboratory, Department of Engineering Design, Indian Institute of Technology Madras, Chennai, Tamil Nadu, India

^c The Systems Realization Laboratory @ OU
University of Oklahoma, Norman, OK, USA

ABSTRACT

Achieving targeted product performance requires the integrated exploration of design spaces across multiple levels of decision-making in systems comprising products, materials, and manufacturing processes - Product-Material-Manufacturing Process (PMMP) systems. This demands the capability to co-design PMMP systems, that is, share ranged sets of design solutions among distributed product, material, and manufacturing process designers. PMMP systems are subject to uncertainties in processing, microstructure, and models employed. Facilitating co-design requires support for simultaneously exploring high-dimensional design spaces across multiple levels under uncertainty.

In this paper, we present the **Co-Design Exploration of Multilevel PMMP systems under Uncertainty** (**CoDE-MU**) framework to facilitate the simultaneous exploration of high-dimensional design spaces across multiple levels under uncertainty. The CoDE-MU framework is a machine learning-enhanced, robust co-design exploration framework that integrates robust, coupled compromise Decision Support Problem (*rc-cDSP*) construct with interpretable Self-Organizing Maps (*iSOM*). The framework supports multidisciplinary designers to i) understand the multilevel interactions, ii) identify the process mechanisms that affect material and product responses, and iii) provide decision support for problems involving many goals with different behaviors across multiple levels and uncertainty.

We use an industry-inspired hot rod rolling (HRR) steel manufacturing process chain problem to showcase the CoDE-MU framework's efficacy in facilitating the simultaneous exploration of the product, material, and manufacturing process design spaces across multiple levels under uncertainty. The framework is generic and facilitates the co-design of multilevel PMMP systems characterized by hierarchical product-material-manufacturing process relations and many goals with different behaviors that must be realized simultaneously at individual levels.

Keywords: Co-design, Robust design, coupled-compromise Decision Support Problem (c-cDSP) construct, interpretable Self-Organizing Map (iSOM)

GLOSSARY

Product-Material-Manufacturing Process (PMMP) system: We define PMMP systems as systems comprising the product, its materials, and associated manufacturing processes.

Design Level: We define ‘design level’ as the interface where design decisions are made by disciplinary experts regarding products, materials, and manufacturing processing, considering their interactions. The disciplinary experts correspond to the product, materials, and process designers, respectively.

Robust satisficing solutions: Solutions that are relatively insensitive to uncertainties and satisfy the designer's requirements.

Co-design: We define co-design from an ICME perspective as a design that supports distributed disciplinary experts, such as product, material, and process designers, across multiple levels of decision-making to work collaboratively in ensuring PMMP system performance. In co-design, designers are supported in i) making decisions simultaneously across multiple levels while considering their interrelations and ii) managing design conflicts to ensure collaboration.

¹ Corresponding author, Email: anellippallil@fit.edu

A previous version of this paper was presented at the TMS ICME 2023 Conference.

53 **Robust Co-design:** We define robust co-design from an ICME perspective as a co-design that supports
54 designers across multiple levels to manage inherent uncertainties by facilitating the identification of a ranged
55 set of common robust satisfying solutions across the levels.

56
57 **NOMENCLATURE AND LIST OF SYMBOLS**

58 [C]	- Carbon concentration
59 c-cDSP	- coupled-compromise Decision Support Problem
60 cDSP	- compromise Decision Support Problem
61 C_{eq}	- Equivalent Carbon
62 CoDE-MU	- Co-Design Exploration of Multilevel PMMP systems under Uncertainty
63 CR	- Cooling Rate
64 [Cu]	- Copper concentration
65 DBD	- Decision-Based Design
66 DCI	- Design Capability Index
67 DSIDES	- Decision Support In the Design of Engineering Systems
68 DSP	- Decision Support Problem
69 D_a	- Ferrite Grain Size
70 d_γ	- Austenite Grain Size
71 EMI	- Error Margin Index
72 GoID	- Goal-oriented Inverse Design
73 HRR	- Hot Rod Rolling
74 HV	- Hardness
75 ICME	- Integrated Computational Materials Engineering
76 IDEM	- Inductive Design Exploration Method
77 iSOM	- interpretable Self-Organizing Map
78 [Mn] and $[Mn_{copy}]$	- Manganese concentration
79 MDO	- Multi-Disciplinary Optimization
80 [N]	- Nitrogen concentration
81 p	- Pearlite colony size
82 [P]	- Phosphorus Concentration
83 PMMP	- Product, Material, and Manufacturing Process
84 PSPP	- Processing-microStructure-Property-Performance
85 rc-cDSP	- robust, coupled-compromise Decision Support Problem
86 SOM	- Self-Organizing Maps
87 [Si]	- Silicon concentration
88 S_0	- Pearlite interlamellar spacing
89 t_{carb}	- Carbide thickness
90 T_{mf}	- Average Austenite to Ferrite transition temperature
91 TS	- Tensile Strength
92 X_f	- Ferrite fraction
93 $X_{f_{eq}}$	- Equivalent Ferrite fraction
94 YS	- Yield Strength
95 ε_r	- Residual strain at the end of rolling

96
97 **1. FRAME OF REFERENCE**

98 The achievement of targeted product performance requires careful consideration of the relations among
99 products, their materials with respective microstructures, and associated manufacturing processing. Product
100 performances are defined by many property requirements with different behaviors that need to be realized
101 simultaneously. The manufacture of steel rods through the hot rod rolling (HRR) manufacturing process
102 chain [1] is an example that illustrates the relations among manufacturing processing, material
103 microstructure, and product properties and performance. In the HRR of steel, cast steel billets are reheated
104 and subsequently processed in rolling and cooling mills to produce hot-rolled steel rods as products. The
105 mechanical properties of the hot-rolled steel rods identify their performance. The steel microstructure
106 determines the mechanical properties. The steel microstructure is influenced by the thermo-mechanical
107 processing that steel billets undergo. Given the relations among manufacturing processing, material
108 microstructure, and product properties and performance, realizing targeted product performance requires a

109 collective consideration of a system comprising the products, materials, and manufacturing processes [2],
 110 referred to as *Product-Material-Manufacturing Process (PMMP) systems* in this paper. This necessitates an
 111 integrated, top-down, systems-based approach for designing PMMP systems, starting with the property
 112 requirements and inversely designing the material microstructure and processing paths to realize the targeted
 113 product performance [3]. Olson's Processing-microStructure-Property-Performance (PSPP) relations [4] lay
 114 the foundation for the inverse, systems-based design of PMMP systems by connecting the product, materials,
 115 and manufacturing processes, as depicted in Figure 1. According to the PSPP relations, the processing during
 116 manufacturing determines the material microstructure and properties, which in turn determines the product
 117 properties and performance.

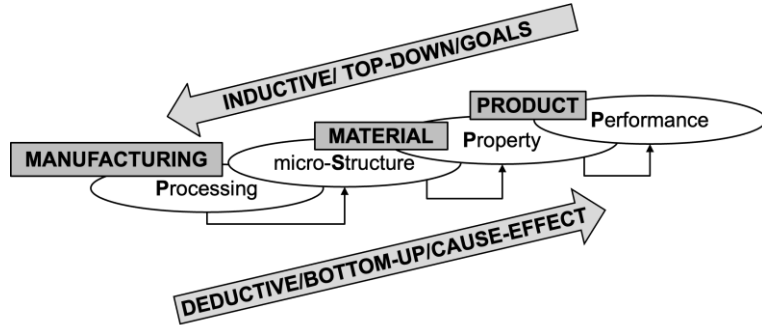


FIGURE 1. Olson's Processing-microStructure-Property-Performance (PSPP) relations [4] that connect products, materials, and manufacturing processes.

118 The design of PMMP systems involves decision-making by different disciplinary experts, such as
 119 product, material, and process designers. The expert decisions are made across multiple levels of a decision
 120 hierarchy defined based on the PSPP relations. The decisions at individual levels in the PMMP system are
 121 directed toward simultaneously achieving their design goals with different behaviors. The difference in
 122 behaviors necessitates the trade-offs or compromises among the goals. Individual-level decisions require
 123 careful consideration of the level-specific constraints and design variable bounds. The individual-level
 124 decisions collectively determine product performance. Due to their interrelations, decisions at an individual
 125 level will affect the decisions at another interrelated level, impacting product performance. Individual-level
 126 decisions can result in 'design conflicts when made in isolation without considering their interrelations.' We
 127 consider design conflicts as situations where the goal-directed decisions at an individual level do not align
 128 with the goal-directed decisions at another interrelated level. Design conflicts will result in poor PMMP
 129 system performance and products not meeting targeted performance requirements. In this paper, we focus on
 130 the simulation-supported design of PMMP systems that help reduce dependency on expensive and time-
 131 consuming lab-scale experimentation and plant trials [5]. The Integrated Computational Materials
 132 Engineering (ICME) initiative [6] provides a heading for simulation-supported PMMP systems design. ICME
 133 focuses on the simulation-supported, concurrent, top-down design of products and materials by using the
 134 PSPP relations to link materials models across multiple length and time scales. According to McDowell [7],
 135 simulation-supported systems design approaches should enhance the designer's understanding of complex
 136 relations in the system to help make informed decisions. The decisions in simulation-supported PMMP
 137 system design are based on simulation-generated information. In simulations, designers use models that are
 138 incomplete, inaccurate, and abstractions of underlying physical phenomena [8] and therefore, they embody
 139 uncertainty. The decisions at individual levels are also subject to design variable uncertainties arising from
 140 random variations in manufacturing processing and material microstructure. These inherent uncertainties
 141 adversely impact the decisions at individual levels and PMMP system performance. Therefore, the
 142 simulation-supported integrated design of PMMP systems requires support for i) consideration of the
 143 relations among individual-level decisions, ii) management of design conflicts, and iii) management of
 144 uncertainties. This necessitates the facilitation of 'robust co-design,' allowing designers distributed across
 145 multiple levels to collaborate by supporting i) the consideration of the relations among individual-level
 146 decisions and ii) the management of uncertainties and design conflicts. By facilitating collaboration, the
 147 satisfaction of the level-specific design goals and the PMMP system performance under conditions of
 148 uncertainty is ensured. Collaboration is achieved by supporting 'co-design exploration' - the simultaneous
 149 exploration of the multilevel design spaces to identify a ranged set of common 'robust satisficing solutions'
 150 across levels. Robust satisficing solutions are relatively insensitive to uncertainties and 'satisfy' and 'suffice'
 151 the design requirements.

152 From a systems design perspective, we consider design a goal-oriented, decision-based process
153 supported by simulations. Therefore, we abide by the Decision-Based Design (DBD) paradigm advocated by
154 Mistree and co-authors [9], where designing is considered a decision-making process wherein designers make
155 a series of decisions, some sequentially while others concurrently. The decisions in DBD are modeled using
156 the Decision Support Problem (DSP) technique [9], anchored in the notion of bounded rationality proposed
157 by Herbert A. Simon [10]. The information required to support decisions in DBD is generated using empirical
158 or simulation-driven surrogate models that are abstractions of reality. Therefore, we seek a ranged set of
159 '*satisficing solutions*' [11] that 'satisfy' and 'suffice' the designer's requirements for the many goals of the
160 design problem by exploring the solution space. The use of the compromise Decision Support Problem
161 (cDSP) [12] construct supports exploring satisficing solutions for problems involving many goals with
162 different behaviors, where goal trade-off considerations are essential. Using the coupled cDSP (c-cDSP)
163 construct [13], designers can model interrelated decision problems across multiple levels, with decisions at
164 individual levels requiring trade-offs among the many goals. The design spaces generated by executing the
165 DSP are explored to identify a '*ranged set of satisficing solutions*.' The ranged set of satisficing solutions
166 helps designers identify i) regions of interest in the design space that require further detailed exploration and
167 ii) key design variables and important relations in a system. In this paper, we look at managing uncertainties
168 by designing the system to be relatively insensitive to uncertainties without reducing or eliminating them,
169 termed 'robust design.' Unlike uncertainty mitigation approaches that involve developing 'perfect' models
170 by collecting more data and performing extensive computations to quantify uncertainties, uncertainty
171 management is computationally less expensive. Uncertainty management is achieved by seeking 'robust
172 solutions' that are relatively insensitive to uncertainties. Type I, Type II, and Type III robust designs are
173 discussed in the literature [1] to deal with uncertainties associated with random noise, design variables, and
174 models, respectively. The use of the Design Capability Index (DCI) [14] and Error Margin Index (EMI) [15]
175 robust design indices in conjunction with the DSP construct have been proposed to help identify a ranged set
176 of '*robust satisficing solutions*' for Type I and II robust designs, and Type III robust design, respectively.
177

178 Most current approaches discussed in the literature for the top-down design of PMMP systems are
179 sequential. Adams and co-authors [16] present a framework to support the inverse design of systems
180 involving materials and processes by employing spectral representation to establish invertible relationships
181 between the same. The materials knowledge systems approach is presented by Kalidindi and co-authors [17,
18], where the bi-directional information flow between different length scales is facilitated to support inverse
182 materials design. Ghosh and co-author [19] present a scalable framework for explicit inverse design named
183 probabilistic machine learning for inverse design. The explicit inverse design is modeled in the framework
184 using a conditional invertible neural network. The focus here is on supporting the identification of product
185 designs that meet targeted performance. This is demonstrated in the inverse aerodynamic design of three-
186 dimensional turbine blades. Sui and co-authors [20] present a deep reinforcement learning scheme for
187 automating the inverse design of composite material structures to realize the required properties. The scheme
188 is applied to a two-dimensional composite planar structure design problem to achieve the strongest average
189 structure tensile strength along the primary axes. Chen and co-authors [21] present a machine-learning-based
190 inverse materials design approach that combines generative inverse design networks, backpropagation, and
191 an active learning strategy to support composite materials design. Kumar and co-authors [22] propose a
192 machine learning-based inverse design technique using neural networks to realize metamaterials with desired
193 properties by tailoring the material topologies. Tsai and co-authors [23] and Qian and co-authors [24] present
194 inverse design approaches that combine artificial neural networks and the genetic algorithm to relate
195 processing with product properties and material properties with structure, respectively. The sequential nature
196 of these approaches results in isolated decision-making across individual levels, thereby failing to consider
197 the multilevel relations and resulting in design conflicts that impact the PMMP system performance. The use
198 of multidisciplinary optimization (MDO) [25] approaches, such as analytical target cascading [26],
199 collaborative optimization [27], and bilevel integrated system synthesis [28, 29] for optimizing multilevel
200 systems while considering the multilevel interactions are discussed in the literature. Ituarte and co-authors
201 [30] present a computer-aided expert system where MDO and surrogate models are employed to conduct
202 trade-off exploration and optimization by coupling product design, materials systems, and manufacturing
203 processes. The authors demonstrate the exploration of optimized solutions across the product, material, and
204 manufacturing disciplines for a digital manufacturing scenario to ensure overall system performance.
205 Rigorous and iteratively intensive optimization techniques that involve optimization loops within and
206 between levels are employed in MDO approaches to identify unique single-point solutions at each level. This
207 is especially challenging during design exploration, where the focus is on quickly identifying a set of

208 satisfactory solutions instead of a unique single-point solution [31]. In the optimization formulation employed
209 in MDO approaches, designers assume the perfectness of the models and objective function and the
210 availability of all required information. Given that the models used are abstractions of reality, the objective
211 functions are imperfect, and the information available is incomplete, our focus is on ‘satisficing’ rather than
212 ‘optimizing.’ We therefore seek a ranged set of robust satisficing solutions.

213 Different approaches that support multilevel co-design exploration under uncertainty by identifying
214 robust satisficing solution sets have been discussed in the literature. Choi and co-authors [3] propose the
215 Inductive Design Exploration Method (IDEM) to support the robust co-design of multilevel systems. IDEM
216 involves sequentially identifying and propagating a range of robust solutions among the individual levels.
217 IDEM is limited by the number of design variables that can be considered, discretization errors, increased
218 computational expense for improved accuracy, and limited flexibility in design, as discussed in [1].
219 Nellippallil and co-authors [1] present an inverse robust design approach named Goal-oriented Inverse
220 Design (GoID) to address some of the limitations in IDEM and support the co-design of systems composed
221 of hierarchically connected products, materials, and associated manufacturing processes. The GoID approach
222 supports sequential design space exploration at the individual levels to identify robust satisficing solutions
223 and their propagation as targets inversely along the hierarchical process chain. The GoID approach does not
224 support the management of design conflicts that can arise due to the sequential nature of design space
225 exploration. To address this shortcoming, Baby and Nellippallil [32] present an information-decision
226 framework to support the systematic detection and management of design conflicts. This is achieved by
227 controlling the design space and decisions across different levels of decisions made sequentially. The IDEM,
228 GoID approach, and the information-decision framework presented by Baby and Nellippallil do not support
229 the simultaneous exploration of the individual levels.

230 Our focus in this paper is on providing decision support during the simulation-supported design of
231 multilevel PMMP systems under uncertainty. From a DBD perspective, we hypothesize that this can be
232 achieved by facilitating robust co-design using a decision support framework that supports i) modeling the
233 level-specific decision problems and their interactions with other levels in PMMP systems in terms of the
234 flow of information, ii) consideration of uncertainties in the decision problems, and iii) co-design exploration
235 of the multilevel design spaces to identify common robust satisficing solutions and thereby manage design
236 conflicts. Given the many design goals at individual levels that require trade-offs and the interactions of
237 decisions across levels, we model the individual-level decision problems and their interaction in PMMP
238 systems using the c-cDSP construct discussed in Section 3.1.1. A combination of Preemptive and
239 Archimedean formulations is used in the c-cDSP. Using the Preemptive formulation, designers can consider
240 the interrelations among the decision problems across multiple levels of a decision problem. Using the
241 Archimedean formulation, designers can consider many goals that require trade-offs at individual levels of a
242 multilevel decision problem. By combining the two, designers can use a coupled DSP formulation to account
243 for many design goals at individual levels and hierarchical relations across levels of a multilevel decision
244 problem. The EMI and DCI robust design indices presented in Section 3.1.2 are combined with the c-cDSP
245 construct to establish the robust, coupled cDSP (rc-cDSP) that helps designers generate robust design
246 solutions across multiple levels. The design spaces across the multiple levels in the PMMP system are
247 visualized in an integrated manner using the interpretable Self Organizing Maps (iSOM) [33] discussed in
248 Section 3.1.3. The integrated iSOM visualization facilitates co-design exploration to identify common robust
249 satisficing solution sets across multiple levels. In this paper, we present the **Co-Design Exploration of**
250 **Multilevel PMMP systems under Uncertainty (CoDE-MU)** framework that enables designers to i) model
251 decision problems at individual levels and their interactions, ii) consider uncertainties, and iii) visualize and
252 efficiently explore multilevel design spaces simultaneously to support robust co-design. The CoDE-MU
253 framework’s novelty lies in two aspects: a) support for modeling multilevel design problems characterized
254 by the need to consider trade-offs among many goals at individual levels and interactions across levels, using
255 a coupled decision problem formulation. This is achieved by combining the Preemptive and Archimedean
256 formulations in the c-cDSP; b) support for the joint management of design conflicts and uncertainties across
257 multiple levels through co-design exploration. Co-design exploration involves the simultaneous exploration
258 of multilevel design spaces. It is realized by exploiting the inherent interpretability and correlated nature of
259 the iSOM plots to help designers efficiently identify common robust satisficing solutions.

260 A description of the problem is presented in Section 2. In Section 3, the CoDE-MU framework to support
261 the robust co-design exploration of multilevel PMMP systems is presented. In Section 4, we showcase the
262 framework’s efficacy in supporting the simultaneous exploration of design spaces across multiple levels in
263 PMMP systems and managing uncertainties using an industry-inspired steel manufacturing process chain test

264 problem – the HRR of steel. In the HRR problem, we focus on the interactions between the material and
 265 cooling process designers at different levels. We end the paper with our key findings and closing remarks in
 266 Section 5. In Appendix A, we present the empirical models that relate the design variables and goals in the
 267 coupled HRR problem.

268

269 2. PROBLEM DESCRIPTION: ACCOUNTING FOR INTERACTIONS ACROSS MULTIPLE 270 LEVELS AND UNCERTAINTIES INVOLVED IN THE DESIGN OF PMMP SYSTEMS

271 The design of PMMP systems involves decisions by the product, materials, and process designers
 272 regarding the product, its materials, and associated manufacturing processes, respectively. The product
 273 designer makes decisions regarding the properties that define the product performance; the materials designer
 274 makes decisions regarding material microstructure and composition that defines material properties; and
 275 process designers make decisions regarding material processing and input material characteristics that
 276 determine the end of processing material microstructure. The interrelated decisions are made across multiple
 277 design levels in a design hierarchy defined by the PSPP relations, as depicted in Figure 2.

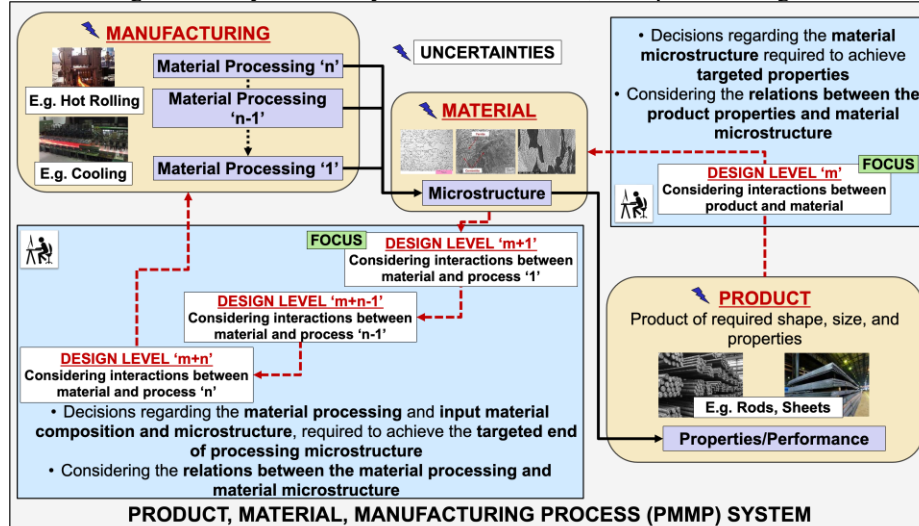


FIGURE 2: Design of PMMP system: Multilevel nature of the PMMP system considering the multiple levels of decisions, multilevel interactions, and uncertainties across the multiple levels. The black arrows depict the forward flow of material, and the red dashed arrows represent the inverse flow of information across multiple design levels that connect the manufacturing processing, material, and product.

278 In Figure 2, Design Level 'm' involves decisions by the materials designer at the top of the hierarchy,
 279 followed by the various process designer's decisions across Design Levels 'm+1' to 'm+n.' Design Levels
 280 'm+1' to 'm+n' are related to the corresponding material processing '1' to 'n' during manufacturing. In this
 281 paper, for demonstration purposes, we focus on the interactions between the Design Levels 'm' and 'm+1'
 282 of the design hierarchy, where $m = 1$. At Design Level 'm' or '1'- the upper level, decisions are made
 283 regarding the material microstructure required to achieve targeted properties by considering the relations
 284 between the product properties and material microstructure. At the lower level - Design Level 'm+1' or '2',
 285 decisions are made regarding the input material composition and microstructure and the processing during
 286 manufacturing process '1' required to achieve the targeted microstructure. This requires considering the
 287 relations between the material processing '1' and the material microstructure. Decisions at Design Level 1
 288 will influence the decisions at Design Level 2. Sequential decision-making across the individual levels in an
 289 isolated manner will result in design conflict, where decisions at Design Level 1 regarding the material
 290 microstructure required to achieve the targeted property goal values may not be achievable at Design Level
 291 2, given the resource constraints. Resource constraints at Design Level 2 are defined in terms of process
 292 limitations and compositional or microstructural characteristics of the input material. The design conflict will
 293 result in targeted product performance not being achieved. Hence, the collective consideration of the
 294 decisions across the individual levels is vital to account for their interactions and manage design conflicts,
 295 thereby ensuring targeted product performance during PMMP systems design. This necessitates co-designing
 296 the individual levels, where designers at different levels are supported in identifying and sharing ranged sets
 297 of design solutions across the levels. Co-design requires support for simultaneously exploring the design

298 spaces across the individual levels. The decisions at the individual levels are subject to various uncertainties
 299 associated with the models employed and other random variations stemming from manufacturing processing
 300 and material microstructure. Therefore, management of these uncertainties during PMMP systems design is
 301 also essential. This can be achieved by facilitating the identification of *robust satisficing solutions*. In this
 302 paper, we specifically focus on uncertainties associated with the design variables and models. Overall, the
 303 need in designing PMMP systems is the support for *simultaneous multilevel design exploration to identify a*
 304 *ranged set of common robust satisficing solutions* across multiple levels.
 305

306 3. A FRAMEWORK TO FACILITATE ROBUST CO-DESIGN EXPLORATION OF 307 MULTILEVEL PMMP SYSTEMS

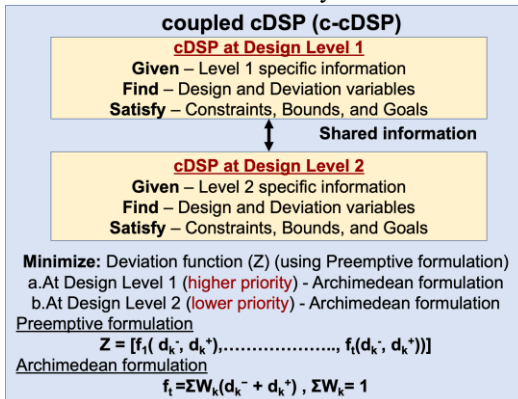
308 In this section, we present a framework, namely Co-Design Exploration of Multilevel PMMP systems
 309 under Uncertainty (CoDE-MU), that supports designers in simultaneously exploring design spaces across
 310 multiple levels to identify a ranged set of common robust satisficing solutions. Using the CoDE-MU
 311 framework, we facilitate the co-design of multilevel PMMP systems that involve the product, materials, and
 312 manufacturing processes while considering the uncertainties. We begin this section by discussing the various
 313 constructs and tools employed in the framework. This is followed by a discussion on decision support using
 314 the framework.

315 3.1. Constructs and tools used in the CoDE-MU framework

316 Three primary constructs and tools are employed in the CoDE-MU framework. They are i) the coupled-
 317 cDSP (c-cDSP) construct, ii) Robust design constructs – DCI and EMI, and iii) the iSOM visualization tool.
 318 A discussion of the constructs and tools follows.

319 3.1.1. c-cDSP construct

320 The coupled DSP [13] is a DSP construct that supports designers to account for the relations among
 321 decisions made hierarchically or concurrently across multiple levels. Using the coupled DSP construct, the
 322 relations among the decisions at different levels are modeled as either a vertical or horizontal coupling [13].
 323 Vertical coupling is used for hierarchical decisions, and horizontal coupling is used for concurrent decisions.
 324 Decisions at individual levels are directed towards simultaneously meeting many design goals with different
 325 behaviors, requiring trade-offs to be made. Hence, we use a c-cDSP to model the multilevel decisions and
 326 their relations in PMMP systems. In c-cDSPs, the level-specific information regarding design variables,
 327 design goals, and constraints is captured using the keywords – *Given*, *Find*, and *Satisfy*, as depicted in Figure
 328 3. Figure 3 depicts the basic structure of the c-cDSP for a system with two levels, Design Levels 1 and 2.



329 **FIGURE 3: The basic structure of the coupled cDSP (c-cDSP) construct**

330 The focus in utilizing the c-cDSP is to find solutions that *minimize* the total deviation of all the design
 331 goals in the system from their target values, termed the '*deviation function*'. Based on the coupling between
 332 the individual levels, the deviation function in c-cDSPs is modeled using a combination of Preemptive and
 333 Archimedean formulations. Using the Preemptive formulation, designers can consider the relations among
 334 decisions made sequentially across multiple levels of a decision hierarchy. Since the decisions in PMMP
 335 systems are made sequentially across different levels of a decision hierarchy defined by the PSPP relations,
 336 the Preemptive formulation is used to model the relations across design levels. In the preemptive formulation,
 337 the goals at different design levels are ordered into different priority sets, as depicted in Figure 3. The priority
 338 sets are ordered according to the position of the design level in the decision hierarchy. The design goals are
 339 satisfied in the order of priority sets, with goals at a higher priority set being met first before meeting the
 goals at a lower priority set [12]. The use of the Preemptive formulation, therefore, allows designers to i)

340 consider the relations among decisions made sequentially across different levels of a decision hierarchy and
 341 ii) assign different priorities for the design goals at different levels. Designers can use the Archimedean
 342 formulation to consider many design goals requiring trade-offs at individual levels in a multilevel decision
 343 problem. In the Archimedean formulation, design goals in a priority set are assigned different weights to
 344 account for the differences in their relative importance [12]. The weights assigned are values between 0 and
 345 1, summing to 1, with a higher value indicating a higher preference. Hence, the Archimedean formulation is
 346 used at individual levels of a multilevel decision problem. By combining the Preemptive and Archimedean
 347 formulations in the proposed framework, designers can account for many design goals requiring trade-offs
 348 at individual levels and relations across levels in PMMP systems using a c-cDSP. The c-cDSP is created and
 349 executed using the Decision Support In the Design of Engineering Systems (DSIDES) platform.

350 3.1.2. Robust design constructs: DCI and EMI

351 The DCI and EMI constructs help designers manage uncertainties by facilitating the identification of
 352 robust solutions that are relatively insensitive to uncertainties. Using the DCI construct [14], designers can
 353 account for design variable uncertainties arising from manufacturing processing and material microstructure
 354 variability. Using the EMI construct [15], designers can consider uncertainties in the models that interrelate
 355 processing with microstructure and microstructure with properties. The ‘larger-is-better’ and ‘smaller-is-
 356 better’ cases for EMI and DCI computations are depicted in Figures 4a and 4b, respectively.

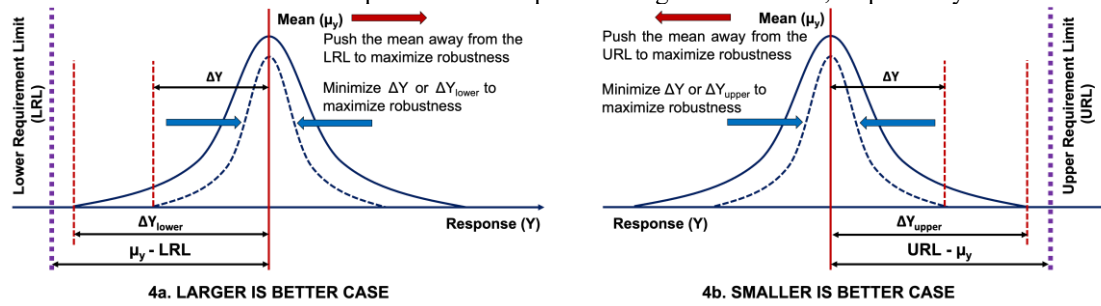


FIGURE 4: Uncertainty in responses with variability in design variables and models for the larger-is-better and smaller-is-better cases. The solid and the dashed bell curves represent different models for a response, indicating variability in the models.

357 Identifying solutions with values of $DCI \geq 1$ and $EMI \geq 1$ will ensure system robustness to uncertainties.
 358 The higher the DCI or EMI values, the higher the safety measure against failure due to uncertainties. A larger-
 359 is-better case is employed for maximization goals. The DCI and EMI values for the larger-is-better case are
 360 computed using Equations 1 and 4, respectively. For the larger-is-better case depicted in Figure 4a, higher
 361 EMI and DCI values can be achieved by i) keeping the mean response (μ_y) as far away as possible from a
 362 lower requirement limit (LRL), thereby maximizing the numerator, and ii) minimizing the spread of the
 363 response - ΔY or ΔY_{lower} , thereby minimizing the denominator. A smaller-is-better case is employed for
 364 minimization goals. The DCI and EMI values for this case are computed using Equations 2 and 5,
 365 respectively. For the smaller-is-better case depicted in Figure 4b, higher EMI and DCI values can be achieved
 366 by i) keeping the mean response (μ_y) as far away as possible from an upper requirement limit (URL), thereby
 367 maximizing the numerator and ii) minimizing the spread of the response - ΔY or ΔY_{lower} , thereby minimizing
 368 the denominator.

369 For the larger-is-better case

$$DCI = \frac{\mu_y - LRL}{\Delta Y} \quad (1)$$

370 For the smaller-is-better case

$$DCI = \frac{URL - \mu_y}{\Delta Y} \quad (2)$$

371 where,

372 ΔY - response variation for small variations in design variables

373 μ_y - Mean responses

374 LRL - Lower requirement limit

375 URL - Upper requirement limit

376 The value of ΔY is computed as per Equation 3.

$$\Delta Y = \sum_{i=1}^r \left| \frac{\partial f}{\partial x_i} \right| * \Delta x_i \quad (3)$$

377 where,

378 $i = 1, 2, 3, \dots, r$ (index of design variables)

379 Δx_i – variation or uncertainty in design variable x_i

380 $\frac{\partial f}{\partial x_i}$ – variation in the response f with respect to the design variable x_i

381 For the larger-is-better case

$$EMI = \frac{\mu_y - LRL}{\Delta Y_{lower}} \quad (4)$$

382 For the smaller-is-better case

$$EMI = \frac{URL - \mu_y}{\Delta Y_{upper}} \quad (5)$$

383 where,

384 μ_y – mean responses,

385 LRL – Lower requirement limit

386 $\Delta Y_{lower} = f_o(x) - Y_{min}$

387 $f_o(x)$ – mean response model

388 $Y_{min} = \text{Min}[f_j(x) - \Delta Y_j]$

389 $j = 0, 1, 2, \dots, s$ (number of uncertainty bounds)

390 $i = 1, 2, 3, \dots, r$ (index of design variables)

391 Δx_i – variation or uncertainty in design variable x_i

392 ΔY_j is the response variation for small variations in design variables for each uncertainty bound j
393 and is computed as per Equation 6.

$$\Delta Y_j = \sum_{i=1}^r \left| \frac{\partial f_j}{\partial x_i} \right| * \Delta x_i \quad (6)$$

394 Given that the required data is available, an approach to generate the upper, mean, and lower bound
395 models is presented in [34]. A discussion of this approach is beyond the scope of this paper. We do not
396 employ the above approach in this paper. Instead, we assume the availability of the upper, mean, and lower
397 bound models to demonstrate the facilitation of model uncertainty management using the framework.

398 3.1.3. iSOM visualization tool

399 iSOM [33] is a tool to visualize high-dimensional data using 2D plots. It is an unsupervised machine-
400 learning algorithm, specifically an artificial neural network, and is a modified form of the conventional Self
401 Organizing Maps (SOM) [35]. SOM, an artificial neural network developed by Kohonen [36], is an efficient
402 algorithm for visualizing multidimensional numerical data [37]. The modification to conventional SOM
403 results in the avoidance of self-intersections and makes the iSOM plots inherently interpretable. iSOM has
404 distinct advantages, such as scalability and interpretability, making it suitable for exploring design space in
405 real-world problems. Plots generated using iSOM are valuable for visualizing the underlying relationships
406 between input design variables and output responses, as depicted in Figure 5 for the function $Z = X^2 + Y^2$.

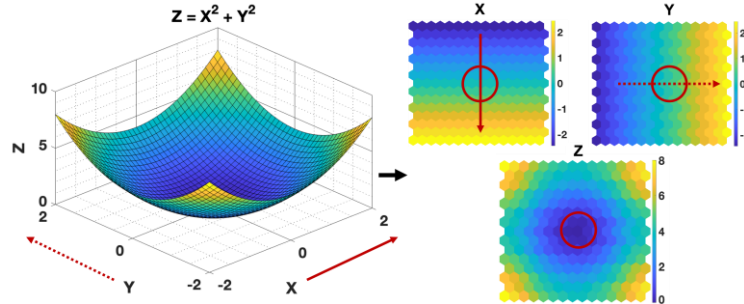


FIGURE 5: Example of visualization using iSOM for a function $Z = X^2 + Y^2$ (plot on the left) with input component plots X and Y and output component plot Z [38]

407 In Figure 5, the arrows in the X and Y component plots represent the increasing direction of the axes
 408 values. Correspondingly, the Z component plot captures the expected trend of a decrease followed by an
 409 increase in Z values with increasing X and Y values. Similarly, suppose designers are interested in the region
 410 the circle identifies in the Z component plot. They can determine the X and Y values that result in the chosen
 411 Z values. The circles in the X and Y component plots in Figure 5 identify these X and Y values. Using the
 412 iSOM plots, designers can carry out forward design space exploration to relate inputs to outputs and inverse
 413 design space exploration to relate outputs to inputs. It is worth noting that the shape of the function remains
 414 consistent in the Z component plot. A detailed discussion of selecting regions of interest using iSOM plots,
 415 regardless of the number of dimensions, is presented in [33]. The work by Sushil and co-authors [38]
 416 showcases the utility of the iSOM tool in visualizing i) high-dimensional design spaces and ii) the relations
 417 between inputs and outputs in multilevel systems. In recent literature, iSOM has been demonstrated as a
 418 potent visualization tool for effectively addressing multi-objective, multi-dimensional, and multi-criteria
 419 problem scenarios. More details can be found in [39-41]. In the proposed framework, we use iSOM to support
 420 the co-design exploration of the multilevel design spaces in PMMP systems by simultaneously visualizing
 421 the design spaces across individual levels using iSOM plots. The iSOM tool is available as a MATLAB code
 422 [33].

423 3.2. Decision support using the CoDE-MU framework

424 In this section, the structure and use of the CoDE-MU framework are discussed in detail. To demonstrate
 425 the concept, in the CoDE-MU framework presented, we only consider the interactions between two levels in
 426 the PMMP system – Design Levels 1 and 2. The CoDE-MU framework comprises four blocks named A, B,
 427 C, and D, as depicted in Figure 6. A detailed discussion of these blocks follows.

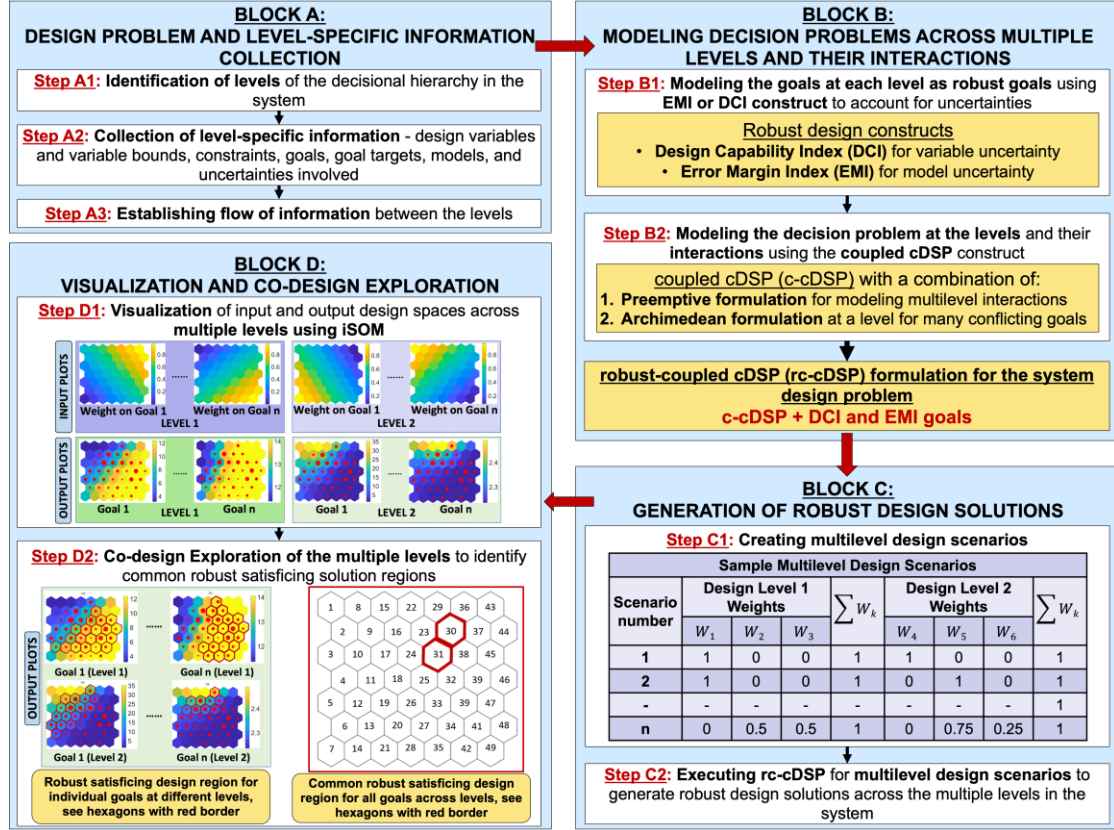


FIGURE 6: Decision support framework to facilitate multilevel robust co-design exploration of PMMP systems (Co-Design Exploration of Multilevel PMMP systems under Uncertainty: CoDE-MU)

428 **Block A:** Design problem and level-specific information collection

429 In Block A, information regarding the multilevel design problem and its levels are collected. Block A
 430 is executed in Steps A1 to A3, as discussed below.

431 **Step A1:** The levels of the decisional hierarchy in the multilevel PMMP system design problem are
 432 identified.

433 Step A2: Information specific to the decision problems at the individual levels is collected. The collected
434 information includes i) design variables – their bounds and uncertainty estimates, ii) models employed and
435 associated uncertainties, iii) design goals and goal targets, and iv) level-specific constraints.

436 Step A3: The flow of information connecting the individual levels is established by identifying shared
437 design variables between levels. A copy of the shared design variables is used as the level-specific design
438 variables at the lower level in the decision hierarchy. Additionally, consistency constraints are established at
439 the lower level to ensure consistency of the shared design variable value at the lower level with the one
440 determined at the upper level.

441 **Block B:** Modeling decision problems across individual levels and their interactions

442 In Block B, the decision problems at various levels in the PMMP system and their interactions are
443 modeled as a single rc-cDSP using the information from Block A, as follows.

444 Step B1: Using the uncertainty information from Step A2, the design goals impacted by uncertainties at
445 the individual levels are formulated as robust goals using the EMI and DCI constructs presented in Section
446 3.1.2. Goals affected by design variable uncertainties are formulated as DCI goals using Equations 1 or 2.
447 Equations 1 and 2 are used when goals are maximization and minimization goals, respectively. Goals
448 impacted by model uncertainties are formulated as EMI goals using Equations 4 or 5. Equations 4 and 5 are
449 used when goals are maximization and minimization goals, respectively. A detailed description of EMI and
450 DCI goal formulations for the HRR test problem is provided in Section 4. Step B1 is followed by Step B2,
451 where the PMMP system design problem is modeled as an rc-cDSP.

452 Step B2: The individual-level decision problems and interactions across different levels in the PMMP
453 system are modeled using the c-cDSP construct. In the c-cDSP, separate instances of the c-DSP construct are
454 used to model decision problems at the individual levels. The keywords of the c-DSP construct – Given,
455 Find, and Satisfy help capture the level-specific information. The interactions between the level-specific
456 cDSPs in the c-cDSP are captured in the form of the flow of shared information, such as shared design
457 variables, as determined in Step A3. In the c-cDSP, the goals impacted by uncertainties are formulated as
458 DCI and EMI goals, as discussed in Step B1. The c-cDSP with EMI and DCI goals is referred to as the rc-
459 cDSP. The deviation function of the rc-cDSP is modeled using a combination of Preemptive and
460 Archimedean formulations. Decisions in PMMP systems are made hierarchically across levels. Hence, the
461 Preemptive formulation is employed, where the design goals at Design Levels 1 and 2 are assigned different
462 priority levels. Design Level 1 decisions are given higher priority as these are made first, followed by Design
463 Level 2 decisions at a lower priority. The difference in preferences among the many design goals at individual
464 levels of a multilevel decision problem is modeled using the Archimedean formulation, where different
465 weights are assigned to the various goals. The weights assigned are values between 0 and 1 that sum up to 1,
466 with higher values indicating higher preference. Combining the Preemptive and Archimedean formulations
467 in the rc-cDSP allows designers to consider many design goals requiring trade-offs at individual levels and
468 relations across levels of a multilevel decision problem, using a coupled decision problem formulation. A
469 detailed description of the rc-cDSP for the HRR test problem is provided in Section 4. The rc-cDSP is created
470 using the DSIDES platform.

471 **Block C:** Generation of robust design solutions

472 In Block C, the rc-cDSP formulation is executed for different multilevel design scenarios using the
473 DSIDES platform to generate robust design spaces across multiple levels. Block C is implemented in two
474 steps.

475 Step C1: The multilevel design scenarios to execute the rc-cDSP are created. The multilevel design
476 scenarios depicted in Step C1, Block C of Figure 6, represent situations with different preferences for the
477 design goals across Design Levels 1 and 2. These multilevel design scenarios are created by combining
478 individual-level design scenarios at Design Levels 1 and 2 in all possible combinations. Individual-level
479 design scenarios are created using Latin hypercube sampling. In each individual-level design scenario,
480 different weights are assigned to the design goals at the level. The weights indicate the difference in
481 preferences amongst the goals. The weights assigned are values between 0 and 1 that add up to 1, with higher
482 values indicating higher preference. If there are ‘n’ distinct design scenarios at an individual level in a
483 multilevel PMMP system with ‘m’ levels, there exist n^m distinct multilevel design scenarios. In this paper,
484 n^2 multilevel design scenarios are considered for the two-level PMMP system.

485 Step C2: The rc-cDSP formulation for the PMMP system is exercised for the n^2 multilevel design
486 scenarios to generate design solutions, including robust solutions, across the levels.

487 **Block D:** Visualization and co-design exploration

488 In Block D, the simultaneous visualization of individual-level solution spaces is carried out using iSOM.
489 This is followed by the co-design exploration of individual-level solution spaces to identify common robust
490 satisficing solutions across multiple levels. Block D is executed in two steps, as detailed below.

491 **Step D1:** The iSOM algorithm is trained for the weight combinations corresponding to different
492 multilevel design scenarios and goal values generated for these scenarios. The trained iSOM algorithm
493 produces separate 2D iSOM plots for each input weight and output goal across multiple levels. The
494 simultaneous visualization of the individual-level solutions spaces across various levels is realized by
495 combining iSOM with the rc-cDSP. The iSOM plots for the output goals help designers visualize the relations
496 between goals across multiple levels.

497 **Step D2:** The solution spaces visualized using iSOM plots are explored to determine satisficing solution
498 regions for the individual goals by setting satisficing limits for each goal. The hexagonal grid points in an
499 iSOM plot whose values meet the set satisficing limit constitute the satisficing solution region for a given
500 goal. For example, in Step D2, Block D of Figure 6, the iSOM grid points with red borders identify the
501 satisficing solution regions for the individual goals. Only the grid points with multilevel design scenarios
502 mapped against them, indicated by the dots on the iSOM grid points, are considered. A larger size of the dot
503 on an iSOM grid point suggests a larger number of multilevel design scenarios being mapped to that specific
504 iSOM grid point. The designers seek to identify common satisficing solution regions for all the goals across
505 the levels by carrying out co-design exploration. Co-design exploration is carried out using a systematic
506 approach described as follows.

507 **Systematic co-design exploration:** Systematic co-design exploration takes place in 3 steps.

508 **Step 1:** Determining if satisficing goal limit relaxations are required.
509 The designer asks, "Does a common satisficing solution region exist for all the goals across the levels?"

- 510 ▪ If "No," the designer proceeds to Step 2.
- 511 ▪ If "Yes," co-design exploration is complete, and common satisficing solutions for all goals across levels
512 are identified.

513 **Step 2:** Identifying a goal to be excluded from satisficing limit relaxation.

514 The designer identifies a goal across the different levels whose satisficing limits cannot be relaxed due
515 to its critical nature. The following goals are candidates to be excluded from satisficing limit relaxation: i)
516 goals formulated as DCIs or EMIs with low satisficing limit values, typically less than 1.5, and ii) other goals
517 deemed critical by designers. All the remaining goals are collectively called 'non-excluded' goals.

518 **Step 3:** Relaxation of satisficing limits for non-excluded goals.

519 The designer begins by grouping all non-excluded goals into two sets: i) Set 1 - All non-excluded goals
520 formulated as DCIs or EMIs with satisficing limit values greater than 1.5, and ii) Set 2 - All remaining non-
521 excluded goals. The relaxation of satisficing limits of non-excluded goals starts with the goals in Set 1,
522 followed by the goals in Set 2.

523 **Step 3a:** Relaxation of satisficing limits for Set 1 goals.

- 524 ▪ The designer picks the goal in Set 1 with the highest satisficing limit defined in terms of DCI
525 or EMI value.
- 526 ▪ For the chosen goal, the designer checks for any common iSOM grid points between the
527 satisficing solution regions of the excluded and chosen goals.
 - 528 ○ If any common iSOM grid points exist, the satisficing limits of the chosen goal are not
529 relaxed. The designer then picks the goal in Set 1 with the next highest DCI or EMI
530 satisficing limit value and repeats the check.
 - 531 ○ If no common iSOM grid points are identified, the designer relaxes the satisficing limit
532 by the least possible amount till common iSOM grid points are identified. The relaxed
533 DCI or EMI satisficing limits can be as low as 1.5.
 - 534 ○ The above step is repeated till all goals in Set 1 are considered.

535 **Step 3b:** Relaxation of satisficing limits for Set 2 goals.

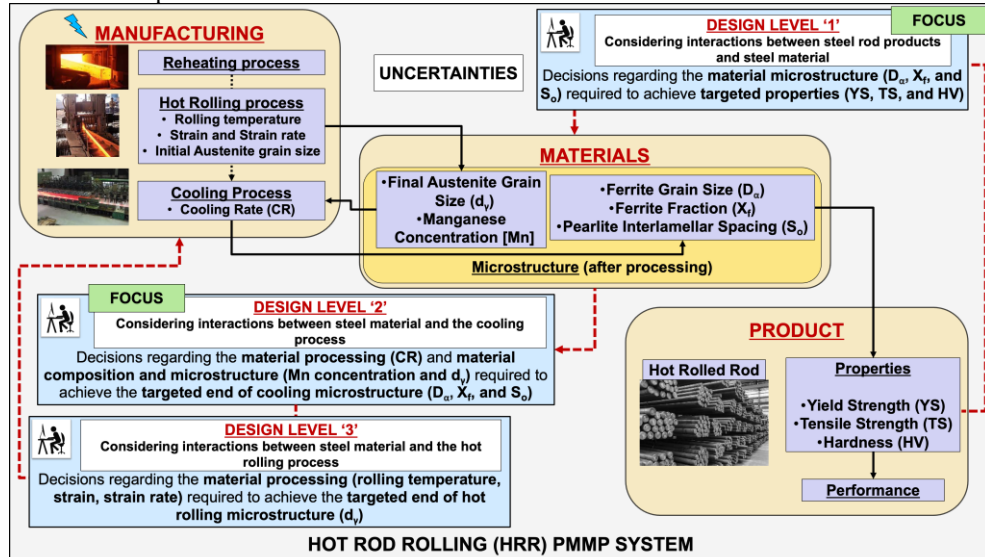
- 536 ▪ Based on the designer's judgment, a goal in Set 2 with a greater scope for satisficing limits
537 relaxation is chosen.
- 538 ▪ For the chosen goal, the designer repeats the procedure to check for common iSOM grid points
539 described in Step 3a until all goals in Set 2 are considered.

540 At the end of Step 3b, designers identify a common satisficing region for all the goals across different
541 levels, as depicted by the plot labeled 'common robust satisficing design region for all goals across levels' in
542 Step D2 of Figure 6. Based on the common region identified, the designer then determines the design
543 scenarios mapped to the common region and the corresponding design variable and goal values. The designer

544 can also use the input and output iSOM component plots to understand the effect of varying the weights and
 545 changing variable values on the goals across multiple levels and other performance indicators in PMMP
 546 systems. In the next section, we demonstrate the CoDE-MU framework's efficacy in supporting the design
 547 of multilevel PMMP systems using an industry-inspired steel manufacturing process chain problem.
 548

549 4. THE HOT ROD ROLLING (HRR) PMMP SYSTEM DESIGN PROBLEM

550 The CoDE-MU framework's efficacy is tested using the industry-inspired Hot Rod Rolling (HRR)
 551 problem. In this problem, we look at the co-design of the HRR PMMP system composed of the hot rolled
 552 rod product, C-Mn steel material, and the cooling manufacturing process. HRR of steel is a complex
 553 manufacturing process chain used to produce hot-rolled steel rods as products. HRR comprises a series of
 554 manufacturing processes executed sequentially, as depicted in Figure 7, starting with the 'reheating process,'
 555 where the primary input steel in the form of billets is reheated. The reheated steel billets are then plastically
 556 deformed to steel rods in the 'hot rolling process' by passing the material through several rollers in rolling
 557 mills. Further, the 'cooling process' is carried out where rolled products are cooled in a run-out table to
 558 produce steel rods as products.



559 **FIGURE 7: Multilevel decision-making and their interrelations in the HRR PMMP system**

560 The above thermo-mechanical processing during manufacturing causes microstructural evolution and
 561 macrostructural changes in the material, resulting in hot-rolled steel rods with specific microstructural
 562 characteristics and corresponding mechanical properties. The performance requirements of the steel rods are
 563 identified in terms of the target mechanical properties of the rods. Realizing hot rolled rods with targeted
 564 performance requires the collective consideration of i) manufacturing processing, ii) material microstructure
 565 and composition, and iii) product properties. In this paper, to demonstrate the efficacy of the CoDE-MU
 566 framework, we bound the HRR PMMP system design problem to consider only the cooling process in the
 567 HRR process chain. The design of the HRR PMMP system using the CoDE-MU framework is discussed
 568 below.

569 **Block A:** The HRR PMMP system and design level-specific information collection.

570 The design of the HRR PMMP system starts at Step A1 in Block A of the CoDE-MU framework.

571 **Step A1:** The levels of decisions in the HRR PMMP system are identified. The design of the HRR PMMP
 572 system involves decisions at three levels – Design Levels 1, 2, and 3, as depicted in Figure 7. Design Level
 573 1 involves decisions regarding materials that affect product properties and performance. Design Levels 2 and
 574 3 involve decisions regarding the cooling and rolling manufacturing processing, respectively, that affect the
 575 material. To demonstrate the efficacy of the CoDE-MU framework, we focus on Design Levels 1 and 2 and
 576 their interactions only. This aspect is clarified in Figure 7 using the block labeled 'FOCUS' beside Design
 577 Levels 1 and 2.

578 **Step A2:** Information specific to Design Levels 1 and 2 is collected. At Design Level 1, decisions are
 579 made regarding i) the steel microstructure design variables identified by the Ferrite grain size (D_a), Ferrite
 580 fraction (X_f), and Pearlite interlamellar spacing (S_o) and ii) the steel composition design variable identified
 by Manganese concentration [Mn] to achieve required mechanical properties for the steel rods. The

581 mechanical property requirements are to achieve targeted Yield strength (YS), Tensile strength (TS), and
 582 Hardness (HV) values of 330MPa, 750MPa, and 170, respectively. The corresponding minimum acceptable
 583 values of 220MPa, 450MPa, and 130 define the lower requirement limits. The YS, TS, and HV property
 584 requirements have different behaviors, and simultaneously realizing these properties requires compromises
 585 or trade-offs. In Appendix A1, the models that relate the mechanical properties to the steel microstructure
 586 and composition design variables at Design Level 1 are listed. The concentration of other elements that
 587 determine the steel composition (Fe, C, Si, N, P, and Cu) is assumed to be fixed. The Design Level 1 specific
 588 information is listed in the Given Section of Table 1.

589 At Design Level 2, decisions are made regarding i) the cooling process design variable - Cooling Rate
 590 (CR), ii) the input steel microstructure design variable - Austenite grain size (d_y), and iii) the input steel
 591 composition design variable - [Mn] to achieve the required end of cooling steel microstructure. The end of
 592 cooling steel microstructure requirements are to achieve the targeted D_a , S_o , and X_f values of 5 μm , 0.15 μm ,
 593 and 1.0, respectively. The acceptable values $D_a = 20\mu\text{m}$, $S_o = 0.2\mu\text{m}$, and $X_f = 0.6$ define the upper
 594 requirement limits for D_a and S_o and the lower requirement limit for X_f . The models that relate the steel
 595 microstructure at the end of cooling to the cooling processing and input material microstructure and
 596 composition design variables at Design Level 2 are provided in Appendix A2. The Design Level 2 specific
 597 information is provided in the Given Section of Table 1.

598 The decisions at Design Levels 1 and 2 are subject to uncertainties associated with design variables. We
 599 consider uncertainty in the model that relates YS to the steel microstructure at Design Level 1 using three
 600 different YS models. Based on the values predicted for YS, we assume the model by Gladman and co-authors
 601 [42] as the mean model - $f_o(x)$ or YS_{mean} , the model by Hodgson and Gibbs [43] as the upper bound - $f_1(x)$
 602 or YS_{upper} , and the model by Kuziak and co-authors [44] as the lower bound model - $f_2(x)$ or YS_{lower} . These
 603 models are presented in Appendix A1. We assume no model uncertainties for the remaining requirements
 604 across Design Levels 1 and 2. The uncertainties associated with the design variables at Design Levels 1 and
 605 2 are listed in the Given Section of Table 1.

606 **Step A3:** The design level-specific information from Step A3 is employed to identify the relationship
 607 between the design levels regarding shared design variables. [Mn] is the shared design variable between
 608 Design Levels 1 and 2. Hence, a copy of this variable, $[Mn_{\text{copy}}]$, is used at Design Level 2 as its level-specific
 609 variables. Additionally, a consistency constraint is imposed at Design Level 2 to ensure that the value of the
 610 [Mn] design variable at both levels remains the same. These details are provided in the Given and Satisfy
 611 Sections of Table 1.

612 **Block B:** Modeling decision problems across multiple levels in the HRR PMMP system and their interactions

613 Using the information from Block A, decisions at Design Levels 1 and 2 and their interactions are
 614 modeled in steps B1 and B2.

615 **Step B1:** Based on the uncertainty information from Step A2, the goals at Design Levels 1 and 2 are
 616 formulated as robust goals using the EMI and DCI constructs. At Design Level 1, the YS requirement is
 617 formulated as an EMI goal to account for uncertainties in the YS model. The formulation of the EMI YS goal
 618 using Equation 3 is discussed below.

$$619 \quad EMI\ YS = \frac{\mu_y - LRL}{\Delta Y_{lower}}$$

620 where,

$$621 \quad LRL = 220\text{MPa}$$

622 μ_y is the YS_{mean} or $f_o(x)$ model in Table A1, Appendix A

$$623 \quad \Delta Y_{lower} = f_o(x) - Y_{min}$$

624 $Y_{min} = \text{Min}[f_j(x) - \Delta Y_j]$, where $j = 0, 1$, and 2 corresponding to the mean, upper and lower bound
 625 models for YS, respectively, in Table A1, Appendix A

$$626 \quad \Delta Y_j = \sum_{i=1}^4 \left| \frac{\partial f_j}{\partial x_i} \right| * \Delta x_i, \text{ where } i = 1, 2, 3, \text{ and } 4 \text{ corresponding to design variables } X_1 \text{ to } X_4 \text{ at Design}$$

627 Level 1, for every $j = 0, 1$, and 2.

628 The TS and HV goals at Design Level 1 are formulated as DCI goals to account for design variable
 629 uncertainties that arise from the variability in steel microstructure - D_a , S_o , and X_f and steel composition
 630 [Mn]. The DCI TS goal formulation using Equation 1 is presented below as an example.

$$632 \quad DCI = \frac{\mu_y - LRL}{\Delta Y}$$

633 where,

634 LRL= 450MPa
 635 μ_y or f is the TS model in Table A1, Appendix A
 636 $\Delta Y = \sum_{i=1}^4 \left| \frac{\partial f}{\partial x_i} \right| * \Delta x_i$, where $i= 1, 2, 3$, and 4 corresponding to design variables X_1 to X_4 at Design
 637 Level 1

638 The D_a , S_o , and X_f goals at Design Level 2 are formulated as DCI goals to facilitate the consideration of
 639 design variable uncertainties that arise from the variability in cooling processing parameter – CR, steel
 640 microstructure - d_γ , and steel composition - $[Mn_{copy}]$. The EMI and DCI goal formulations at Design Levels
 641 1 and 2 are maximization goals to achieve higher EMI and DCI values, thereby ensuring greater robustness
 642 to uncertainties. The EMI YS, DCI TS, and DCI HV goal targets are set as 3, 8, and 8, respectively. The goal
 643 targets for DCI D_a , DCI S_o , and DCI X_f are set as 3, 10, and 10, respectively.

644 Step B2: Using the information from Block A, the decisions at Design Levels 1 and 2 and interactions
 645 are modeled using the c-cDSP construct. In the c-cDSP, a copy of the $[Mn]$ shared design variable and a
 646 consistency constraint are employed at Design Level 2 to account for the interactions, as listed in the Satisfy
 647 Section in Table 1. The DCI and EMI goal formulations from Step B1 are used as goals for the c-cDSP. The
 648 DCI and EMI goals and the c-cDSP together form the rc-cDSP for the HRR PMMP system, as detailed in
 649 Table 1. Further design requirements pertaining to cost or other production considerations may be added as
 650 goals at the appropriate design level in the rc-cDSP. Additionally, constraints, as listed in the Satisfy Section
 651 in Table 1, are established to i) ensure DCI and EMI goal values greater than one and guarantee robust
 652 solutions and ii) to account for any limitations associated with the manufacturing processing. The deviation
 653 function of the rc-cDSP is modeled using a combination of Preemptive and Archimedean formulations. The
 654 decisions in the HRR PMMP system are made hierarchically, with decisions at Design Level 1 being made
 655 before the decisions at Design Level 2. The Preemptive formulation is employed to help account for the
 656 hierarchical relation between Design Levels 1 and 2. The difference in preferences among the many design
 657 goals at the individual levels - Design Levels 1 and 2, is modeled using the Archimedean formulation, as
 658 given in the Minimize Section in Table 1. By combining the Preemptive and Archimedean formulations in
 659 the rc-cDSP, designers can consider many goals at Design Levels 1 and 2 and relations between Design
 660 Levels 1 and 2 in a coupled decision problem formulation.

661 **TABLE 1: Robust coupled cDSP (rc-cDSP) for the HRR PMMP system considering interactions between
 662 Design Levels 1 and 2**

GIVEN	
a. <u>HRR PMMP system information</u>	<p>Constants:</p> <ul style="list-style-type: none"> i. Elemental composition of C-Mn steel: $[Cu]= 0.08\%$; $[P]= 0.019\%$; $[C]= 0.18\%$; $[N]= 0.007\%$; $[Si]= 0.36\%$ ii. Average Austenite to Ferrite transition temperature, $T_{mf}= 700^\circ C$ iii. Pearlite colony size, $p= 6\mu m$, iv. Carbide thickness, $t_{carb}= 0.025\mu m$ v. Residual strain at the end of rolling, $\varepsilon_r= 0$ (assumed)
b. Design variables (x_i), their bound, and uncertainties at Design Level 1	<ul style="list-style-type: none"> i. $0.1 \leq x_1 (X_f) \leq 1.0$ ii. $5 \leq x_2 (D_a) \leq 25 (\mu m)$ iii. $0.15 \leq x_3 (S_o) \leq 0.25 (\mu m)$ iv. $0.7 \leq x_4 ([Mn]) \leq 1.5 (\%)$ (shared) <ul style="list-style-type: none"> • Uncertainty: $D_a= \pm 3\mu m$; $X_f= \pm 0.1$; $S_o= \pm 0.01\mu m$; $[Mn]= \pm 0.1\%$ <p>Design variables (x_i), their bounds, and uncertainties at Design Level 2</p> <ul style="list-style-type: none"> i. $30 \leq x_5 (d_\gamma) \leq 100 (\mu m)$ ii. $0.1833 \leq x_6 (CR) \leq 1.66 (\text{ }^\circ C/\text{s})$ iii. $0.7 \leq x_7 ([Mn_{copy}]) \leq 1.5 (\%)$ (shared) <ul style="list-style-type: none"> • Uncertainty: $d_\gamma= \pm 10\mu m$; $CR= \pm 0.166\text{ }^\circ C/\text{s}$; $[Mn_{copy}]= \pm 0.1\%$
c. <u>End requirements at Design Level 1 in terms of steel rod mechanical properties</u>	<ul style="list-style-type: none"> i. Achieve targeted YS [MPa] ii. Achieve targeted TS [MPa] iii. Achieve targeted HV <p>Corresponding requirement on the rc-cDSP goals (G_k) at Design Level 1 ($k= 1,2,3$)</p>

<ol style="list-style-type: none"> i. Goal G₁: Maximize EMI YS ii. Goal G₂: Maximize DCI TS iii. Goal G₃: Maximize DCI HV <p><u>Goal Targets:</u> G_{1,target} = 3; G_{2,target} = 8; G_{3,target} = 8</p> <p><u>End requirements at Design Level 2 in terms of steel microstructural characteristics</u></p> <ol style="list-style-type: none"> i. Achieve targeted D_α ii. Achieve targeted S₀ iii. Achieve targeted X_f <p><u>Corresponding requirement on the rc-cDSP goals (G_k) at Design Level 2 (k= 4,5,6)</u></p> <ol style="list-style-type: none"> i. Goal G₄: Maximize DCI D_α ii. Goal G₅: Maximize DCI S₀ iii. Goal G₆: Maximize DCI X_f <p><u>Goal Targets:</u> G_{4,target} = 3; G_{5,target} = 10; G_{6,target} = 10</p> <ul style="list-style-type: none"> • The models for the end requirements at Design Levels 1 and 2 are provided in Appendix A1 and A2, respectively. • Uncertainty associated with the YS model is represented by the YS_{mean}, YS_{upper}, and YS_{lower} models listed in Appendix A1.
<p>d. <u>Requirement limits at Design Level 1:</u> Lower Requirement Limit (LRL) for YS_{mean}= 220MPa; LRL for TS= 450MPa; LRL for HV= 130</p> <p><u>Requirement limits at Design Level 2:</u> Upper Requirement Limit (URL) for D_α= 25μm; URL for S₀= 0.25μm; LRL for X_f= 0.5</p>
FIND values of
<p>a. Design variables: X_i, where i= 1,2,3,4,5,6,7</p> <p>b. Deviation variables: d_k⁺ and d_k⁻, where k= 1,2,3,4,5,6</p>
SATISFY
<ol style="list-style-type: none"> a. Design Level 1 constraints <ol style="list-style-type: none"> ii. EMI YS ≥ 1 iii. DCI TS ≥ 1 iv. DCI HV ≥ 1
<u>Design Level 2 constraints</u>
<ol style="list-style-type: none"> i. d_γ≤100 ii. d_γ≥30 iii. CR ≤1.66 iv. CR ≥0.1833 v. Mn_{copy}= Mn (<i>consistency constraint for shared design variable</i>) vi. DCI D_α ≥ 1 vii. DCI S₀ ≥ 1 viii. DCI X_f ≥ 1
<ol style="list-style-type: none"> b. Variable bounds at Design Level 1 <ol style="list-style-type: none"> i. 0.1≤ X_f≤1.0 ii. 5≤ D_α≤25 iii. 0.15≤ S₀≤0.25 iv. 0.7≤ [Mn]≤1.5
<u>Variable bounds at Design Level 2</u>
<ol style="list-style-type: none"> i. 30≤ d_γ≤100 ii. 0.1833≤ CR ≤1.66 iii. 0.7≤ [Mn_{copy}]≤1.5
<u>Deviation variable bounds</u>
d _k ⁺ , d _k ⁻ >= 0 and d _k ⁺ * d _k ⁻ = 0
MINIMIZE
<p>Preemptive formulation at two levels.</p> <p>The deviation function (Z) needs to be minimized.</p> <p style="text-align: center;">Min Z= (f₁, f₂)</p>
<p><u>Priority 1: Design Level 1 (Archimedean Formulation)</u></p> <p style="text-align: center;">f₁= Σ W_k (d_k⁺+ d_k⁻),</p>

where, W_k = weights assigned to the deviations of the individual goals from the target values, $\sum W_k = 1$, and $k = 1, 2, 3$.

Priority 2: Design Level 2 (Archimedean Formulation)

$$f_2 = \sum W_k (d_k^+ + d_k^-),$$

where, W_k = weights assigned to the deviations of the individual goals from the target values, $\sum W_k = 1$ and $k = 4, 5, 6$

663 **Block C:** Generation of robust design solutions across Design Levels 1 and 2

664 The rc-cDSP is executed for various multilevel design scenarios to generate robust design solutions
665 across Design Levels 1 and 2.

666 **Step C1:** Multilevel design scenarios are created by considering all combinations of individual-level
667 design scenarios at Design Levels 1 and 2. Individual-level design scenarios are created by assigning different
668 combinations of weights to the goals at the level using a Latin hypercube sampling (LHS) design. Using the
669 LHS design helps cover the design space effectively. 13 design scenarios are considered at the individual
670 levels, leading to 169 multilevel design scenarios across the two design levels. Some sample multilevel design
671 scenarios are listed in Table 2.

TABLE 2: Sample multilevel design scenarios

Scenario #	Design Level 1 weights ($W_{k=1,2,3}$)				Design Level 2 weights ($W_{k=4,5,6}$)			
	W_1	W_2	W_3	$\sum_k W_k$	W_4	W_5	W_6	$\sum_k W_k$
1	0.33	0.13	0.54	1	0.33	0.13	0.54	1
2	0.33	0.13	0.54	1	0.35	0.42	0.23	1
-	-	-	-	-	-	-	-	-
55	0.16	0.42	0.42	1	0.06	0.06	0.88	1
-	-	-	-	-	-	-	-	-
169	0.33	0.18	0.49	1	0.33	0.18	0.49	1

672 **Step C2:** The HRR PMMP system rc-cDSP is executed for the multilevel design scenarios to generate
673 robust design solutions for the goals across Design Levels 1 and 2.

674 **Block D:** Visualization and co-design exploration of the solution spaces

675 In Block D, the visualization and co-design exploration of the robust solution spaces across Design
676 Levels 1 and 2 is carried out in Steps D1 and D2, respectively.

677 **Step D1:** The weight combinations corresponding to different multilevel design scenarios and goal
678 values generated for these scenarios at Design Levels 1 and 2 are used to train the iSOM algorithm. The
679 trained iSOM helps visualize the solution spaces across the levels simultaneously by generating six iSOM
680 plots for the six goals across Design Levels 1 and 2, as shown in Figure 8.

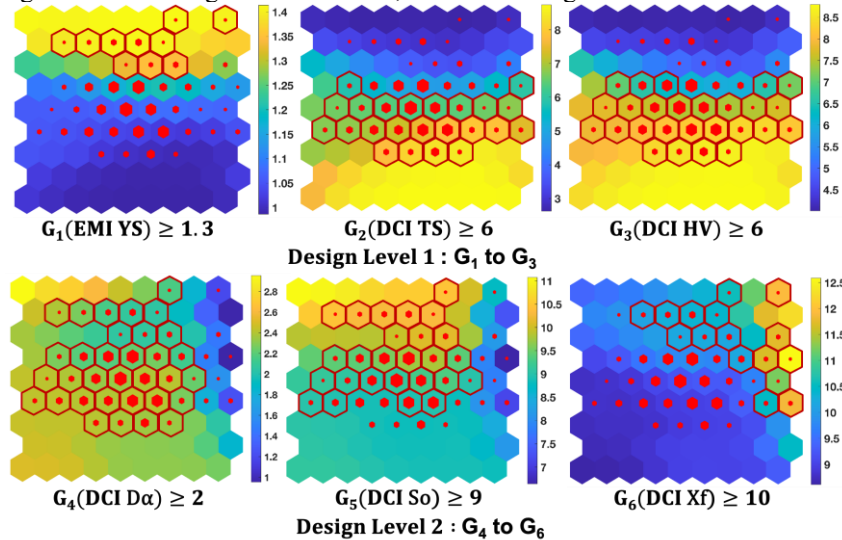


FIGURE 8: Initial iSOM plots for goals at Design Levels 1 and 2, with yellow and dark blue regions representing relatively high and low robustness regions, respectively. The hexagonal iSOM grid points highlighted in red indicate satisfying solutions regions for goals. The red dots indicate design scenarios being mapped to the iSOM grid points.

681 Step D2: The iSOM plots for the goals are used to conduct co-design exploration of Design Levels 1 and
 682 2 by simultaneously exploring the solution spaces. Co-design exploration of the levels helps identify common
 683 robust satisfying solutions for the goals across the two levels.

684 The co-design exploration of Design Levels 1 and 2 begins by establishing the satisfying limits for all
 685 the goals to identify robust satisfying solution regions on the iSOM plots for each goal. The designer focuses
 686 on ensuring greater safety against uncertainties by choosing regions with higher EMI or DCI values. Hence,
 687 the satisfying limits for the goals at Design Levels 1 and 2 are initially set to the higher end of the achievable
 688 EMI or DCI values, as follows.

At Design Level 1

- i. EMI YS, $G_1 \geq 1.3$
- ii. DCI TS, $G_2 \geq 6$
- iii. DCI HV, $G_3 \geq 6$

At Design Level 2

- i. DCI D_α , $G_4 \geq 2$
- ii. DCI S_o , $G_5 \geq 9$
- iii. DCI X_f , $G_6 \geq 10$

689 For the above satisfying goal limits, iSOM grid points highlighted with a red border in Figure 8 indicate
 690 the initial satisfying solution regions.

Systematic co-design exploration

692 Step 1: With the satisfying limits set to the above values, the designer identifies no common region in
 693 terms of iSOM grid points for all six goals across Design Levels 1 and 2. The designer, therefore, proceeds
 694 to Step 2.

695 Step 2: Since all the goals are formulated as EMIs or DCIs, the designer picks the goal with the lowest
 696 satisfying limit as the goal to be excluded from satisfying limit relaxation. Hence, G_1 , with a satisfying limit
 697 of less than 1.5, is picked as the goal to be excluded from the satisfying limit relaxation. G_2 to G_6 constitute
 698 the non-excluded goals.

699 Step 3: The designer groups all non-excluded goals (G_2 to G_6) into Set 1 as they are all formulated as
 700 DCIs or EMIs.

701 Step 3a: The designer picks G_6 with the largest satisfying limit value. Since common grid points with
 702 the excluded goal G_1 are identified, as depicted by the iSOM grid points highlighted in black for G_1 and G_6
 703 in Figure 9, the satisfying limit of G_6 is not relaxed. The designer then picks the goals with the next highest
 704 satisfying limit, G_5 . The designer checks for common grid points and decides not to relax the satisfying limit
 705 for G_5 as common grid points exist. The designer then considers G_3 . Since G_3 has no common iSOM grid
 706 points with the excluded goal G_1 , G_3 's satisfying limit is relaxed to 5. This results in the iSOM grid points
 707 highlighted in black in Figure 9 becoming common for G_3 and G_1 . The above step is repeated for G_2 , resulting
 708 in its satisfying limit being relaxed to 3.5. Finally, the designer considers G_4 with the smallest satisfying
 709 limit in Set 1. Since G_4 has common iSOM grid points with the excluded goal G_1 , G_4 's satisfying limit is not
 710 relaxed.

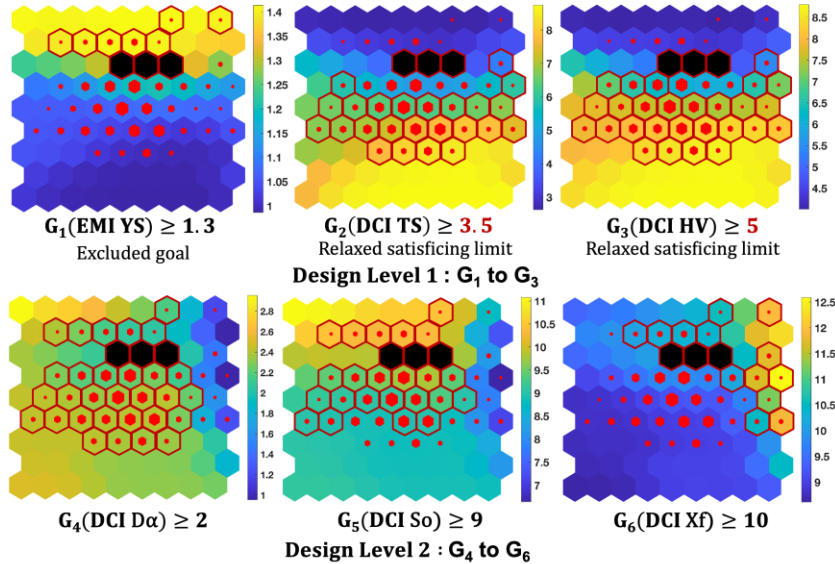


FIGURE 9: iSOM plots for all goals across Design Levels 1 and 2 after systematically updating the satisfying goal limits. The iSOM grid points highlighted in red indicate the satisfying solutions regions for the goals. The black iSOM grid points indicate the common satisfying solution region for all Design Levels 1 and 2 goals.

With the updated satisfying limits, three iSOM grid points are determined to be the common satisfying region for all the goals, as depicted by the black iSOM grid points in Figure 9. These grid points have six design scenarios mapped against them, resulting in six common robust satisfying design solutions across Design Levels 1 and 2 of the HRR PMMP system. Hence, using the combination of the rc-cDSP and iSOM in the CoDE-MU framework, designers can simultaneously explore the solution spaces across Design Levels 1 and 2 to identify common robust satisfying design solutions. The CoDE-MU framework thereby facilitates the robust co-design of the HRR PMMP system. The six design scenarios and the corresponding goal values at Design Levels 1 and 2 are listed in Table 3.

TABLE 3: Common solutions identified after co-design exploration of Design Levels 1 and 2 in the HRR PMMP system

Design Scenario #	Robust goal values					
	Design Level 1			Design Level 2		
	EMI YS	DCI TS	DCI HV	DCI D_a	DCI S_o	DCI X_f
40	1.45	3.25	4.62	2.00	10.40	10.21
44	1.45	3.25	4.62	1.67	9.75	10.84
49	1.45	3.25	4.62	2.00	10.40	10.21
50	1.45	3.25	4.62	1.67	9.75	10.84
52	1.45	3.25	4.62	2.00	10.40	10.21
144	1.45	3.25	4.62	2.00	10.40	10.21

On analyzing the EMI and DCI values in Table 3, all solutions identified are robust with EMI and DCI values greater than 1. The design variables values, steel rod properties, and steel microstructure corresponding to the six common robust satisfying design solutions are listed in Table 4.

TABLE 4: Design variables, properties, and microstructure corresponding to the common robust satisfying solutions identified after co-design exploration of Design Levels 1 and 2 in the HRR PMMP system

Design Scenario #	Design Variables							Properties and Microstructure					
	Design Level 1				Design Level 2			Design Level 1			Design Level 2		
	X_f	D_a	S_o	Mn	d_γ	CR	Mn_{copy}	YS_{mean}	TS	HV	D_a	S_o	X_f
		μm	μm	%	μm	°C/s	%	MPa	MPa		μm	μm	
40	0.52	8.50	0.15	1.50	42.50	1.16	1.50	341.53	617.03	151.23	18.87	0.11	0.67
44	0.52	8.50	0.15	1.50	42.50	0.98	1.50	341.53	617.03	151.23	19.51	0.12	0.68
49	0.52	8.50	0.15	1.50	42.50	1.16	1.50	341.53	617.03	151.23	18.87	0.11	0.67
50	0.52	8.50	0.15	1.50	42.50	0.98	1.50	341.53	617.03	151.23	19.51	0.12	0.68
52	0.52	8.50	0.15	1.50	42.50	1.16	1.50	341.53	617.03	151.23	18.87	0.11	0.67
144	0.52	8.50	0.15	1.50	42.50	1.16	1.50	341.53	617.03	151.23	18.87	0.11	0.67

Upon analyzing the mechanical properties of steel rods listed in Table 4, a mean YS of 341.53MPa, TS of 617.03MPa, and HV of 151.23 are achieved by ensuring a steel microstructure with moderate to high X_f (0.52), low D_a (8.5 μm), low S_o (0.15 μm), and steel composition with [Mn] of 1.5%. At Design Level 2, the cooling process parameter (CR), input steel microstructure (d_γ), and composition ([Mn]) variable values identified help achieve targeted X_f , D_a , and S_o values, given the cooling process constraints and uncertainties involved. This results in D_a values between 18.9 and 19.5 μm , S_o values between 0.11 and 0.12 μm , and X_f values between 0.67 and 0.68, as listed in Table 4. Correspondingly, the cooling rate during the cooling process is identified to be between 0.98 and 1.16°C/s, and the input steel microstructure, d_γ of 42.5 μm . Based on the CR value range, it is evident that higher cooling rates are necessary to realize the required steel microstructure and steel rod properties. Therefore, designers can assess the impact of process variables on the product and materials using the CoDE-MU framework.

From the iSOM plots in Figure 9, the relations among the goals at the individual levels can also be ascertained. For example, at Design Level 1, a focus on achieving high EMI YS, depicted by the yellow regions on the iSOM plot for G_1 , will result in lower DCI TS and DCI HV values, shown by the blue regions on the G_2 and G_3 iSOM plots. Similarly, at Design Level 2, a focus on maximizing DCI X_f , depicted by the yellow regions in the iSOM plot for G_6 , will result in lower DCI S_o and DCI D_a values, shown by the blue regions on the G_4 and G_5 iSOM plots. Moreover, the relations among the goals across levels can also be established based on the iSOM plots. For example, a focus on achieving high DCI S_o and DCI D_a values at

742 Design Level 2, depicted by the yellow regions on the G_4 and G_5 iSOM plots, will result in high EMI YS
743 value, represented by the yellow regions in the G_1 iSOM plot, and low DCI TS and DCI HV values,
744 represented by the blue regions in the G_2 and G_3 iSOM plots, at Design Level 1. Therefore, the CoDE-MU
745 framework also supports designers in understanding the relations within and between levels during the design
746 of the HRR PMMP system.

747

748 5. CLOSING REMARKS

749 Realizing products that simultaneously meet many performance requirements with different behaviors
750 requires careful consideration of the relations among the product, materials, and manufacturing processes
751 across multiple decision levels in PMMP systems. Failure to account for the relations among individual levels
752 will result in design conflicts that will adversely impact the realization of targeted product performance.
753 Uncertainties arising from the variability associated with processing and microstructure and uncertainties in
754 the models employed will also adversely affect product performance. Hence, it is vital to consider the
755 relations among individual levels and manage the design conflicts and uncertainties during PMMP systems
756 design. This necessitates the support for co-design exploration of individual design levels to identify ranged
757 sets of common robust satisfying solutions across the levels.

758 In this paper, we present a decision support framework that facilitates the co-design exploration of
759 multiple levels of the PMMP systems under uncertainty, namely CoDE-MU. In the CoDE-MU framework,
760 the c-cDSP construct is combined with EMI and DCI robust design constructs and machine-learning-based
761 iSOM visualization to facilitate multilevel robust co-design exploration. Using the framework, designers can
762 i) model decision problems across individual levels and their interactions using a coupled decision problem
763 formulation, ii) visualize and simultaneously explore the design spaces across multiple levels, iii) manage
764 the impact of uncertainties, and iv) identify important processing and microstructure variables that influence
765 the product performance. The framework enhances the ability of designers to account for the interactions
766 among the products, materials, and manufacturing processes and, at the same time, manage the inherent
767 uncertainties in PMMP systems. This is achieved by employing the rc-cDSP, where the c-cDSP construct is
768 used with the EMI and DCI robust design constructs. In the rc-cDSP, a combination of the Preemptive and
769 Archimedean formulations is employed to help account for i) the hierarchical relationships among the
770 individual levels and ii) the many design goals requiring trade-offs at individual levels of a multilevel
771 decision problem. Using the framework, designers can perform efficient, robust co-design exploration. This
772 is realized by employing the iSOM visualization tool to simultaneously explore the individual-level design
773 spaces formulated using the rc-cDSP. iSOM visualization involves training iSOM using weight combinations
774 corresponding to multilevel design scenarios of the rc-cDSP and goal values generated for these scenarios.
775 Two-dimensional plots for the output goals across multiple levels are generated via iSOM. Using the
776 simultaneous solution space visualization capability offered by iSOM, designers are further able to explore
777 and seek common robust satisfying regions for the many goals across multiple levels, thereby facilitating
778 co-design and the joint management of design conflicts and uncertainties. The framework supports designers
779 in accounting for various soft and hard requirements across the design levels by facilitating their modeling
780 in the rc-cDSP as goals and constraints, respectively. This allows consideration of any additional
781 requirements relating to cost, production considerations, and process limitations during PMMP system
782 design.

783 The framework's capability in supporting the above functionalities is demonstrated using an industry-
784 inspired steel manufacturing process chain problem – HRR of steel. Using the framework, the co-design of
785 the HRR PMMP system that involves the steel rod product, steel material, and the cooling process at two
786 different levels - Design Levels 1 and 2, their interactions and inherent uncertainties are demonstrated. The
787 design conflicts arising from the hierarchically related levels are managed by simultaneously exploring the
788 solution spaces across Design Levels 1 and 2 to identify common robust satisfying solutions for the goals
789 across the levels. In the HRR test problem, we consider model uncertainties in the YS design goal by
790 assuming different mean, upper, and lower models. We assume that TS and HV functions are not subject to
791 model uncertainties and thus consider their models mean models. The uncertainty associated with the
792 function parameters of TS and HV are considered. This assumption is made to demonstrate the efficacy of
793 the robust design constructs for various sources of uncertainties in the problem, namely model structure
794 uncertainty (via EMI metric) and model parameter uncertainty (via DCI metric). The limitation of such an
795 assumption is that the design solutions found will be sensitive to model variability since models are always
796 abstractions of reality. The formulation of model uncertainty requires designers to have data sets that capture
797 the variability of the function with respect to the design variables. This could be practically difficult for

798 certain materials design problems with limited information. The integrated mean response model and
799 prediction interval approach presented by McDowell and co-authors [34] allows the efficient estimation of
800 the mean function model and prediction intervals, defining the upper and lower bounds if simulation-assisted
801 or experimental data is available. Extending the current framework with efficient data-driven approaches to
802 consider model uncertainty and its propagation across levels is a focus for future research.

803 The generic nature of the framework is made evident by the generic nature of the constructs and tools
804 employed. Using the framework, we facilitate the robust co-design of multilevel PMMP systems
805 characterized by many design goals requiring trade-offs at individual levels and hierarchical relations among
806 the levels. From an ICME perspective, the CoDE-MU framework supports the need to consider the influence
807 of manufacturing processing in materials design. This is achieved by facilitating the consideration of
808 manufacturing processing decisions and their influences during PMMP systems design. The CoDE-MU
809 framework can also facilitate location-specific materials design, a significant focus area in ICME. Location-
810 specific materials design can be realized by supporting the designers to account for the influence of the
811 manufacturing process to tailor material microstructure and properties at desired locations.

812 The proposed CoDE-MU framework can be further expanded to account for all the manufacturing
813 processing decisions and their interactions by modifying the rc-cDSP formulation with additional levels. The
814 changes to the rc-cDSP required to facilitate the same involve creating additional priority levels in the
815 Preemptive formulation of the deviation function. Consequently, the multilevel design scenarios need to be
816 modified to account for the new design levels in the PMMP system.

817 818 ACKNOWLEDGMENTS

819 Anand Balu Nellippallil gratefully acknowledges support from NSF Award 2301808. Mathew Baby and
820 Anand Balu Nellippallil thank the Department of Mechanical and Civil Engineering, Florida Institute of
821 Technology, for the support. Janet K. Allen and Farrokh Mistree gratefully acknowledge the John and Mary
822 Moore Chair and the L.A. Comp Chair at the University of Oklahoma. We acknowledge the support of
823 Akshay Guptan, an undergraduate student at Florida Institute of Technology, for the help in running the
824 coupled cDSP formulation and generating the data for the test problem.

825 826 CONFLICT OF INTEREST STATEMENT

827 On behalf of all authors, the corresponding author states that there is no conflict of interest.

828 829 REFERENCES

- 830 1. Nellippallil, A. B., Allen, J. K., Gautham, B. P., Singh, A. K., and Mistree, F., 2020, "Robust Concept
831 Exploration of Materials, Products, and Associated Manufacturing Processes," *Architecting Robust Co-
832 Design of Materials, Products, and Manufacturing Processes*, Springer International Publishing, pp.
833 263-296.
- 834 2. Arroyave, R., and McDowell, D. L., 2019, "Systems Approaches to Materials Design: Past, Present,
835 and Future," *Annual Review of Materials Research*, vol. 49, no. 1, pp. 103-126.
- 836 3. Choi, H., McDowell, D. L., Allen, J. K., Rosen, D., and Mistree, F., 2008, "An Inductive Design
837 Exploration Method for Robust Multiscale Materials Design," *Journal of Mechanical Design*, vol. 130,
838 no. 3, p. 031402.
- 839 4. Olson, G. B., 1997, "Computational Design of Hierarchically Structured Materials," *Science*, vol. 277,
840 no. 5330, pp. 1237-1242.
- 841 5. The Minerals, Metals & Materials Society, 2015, "Modeling Across Scales: A Roadmapping Study for
842 Connecting Materials Models and Simulations Across Length and Time Scales," *TMS*, Warrendale, PA.
- 843 6. Pollock, T. M., Allison J. E., and co-authors, 2008, "Integrated Computational Materials Engineering:
844 A Transformational Discipline for Improved Competitiveness and National Security," *The National
845 Academies Press*, Washington, DC.
- 846 7. McDowell, D. L., 2018, "Microstructure-Sensitive Computational Structure-Property Relations in
847 Materials Design," *Computational Materials System Design*, Springer International Publishing, pp. 1-
848 25.
- 849 8. Simpson, T., Toropov, V., Balabanov, V., and Viana, F., 2008, "Design and Analysis of Computer
850 Experiments in Multidisciplinary Design Optimization: A Review of How Far We Have Come - Or
851 Not," *12th AIAA/ISSMO Multidisciplinary Analysis and Optimization Conference*, American Institute
852 of Aeronautics and Astronautics, Paper No. 2008-5802.

853 9. Mistree, F., Smith, W., Bras, B., Allen, J., and Muster, D., 1990, "Decision-Based Design: A
 854 Contemporary Paradigm for Ship Design," *Transactions of the Society of Naval Architects and Marine*
 855 *Engineers*, vol. 98, pp. 565–597.

856 10. Simon, H. A., 1947, "Administrative Behavior," *Mcmillan*, New York.

857 11. Simon, H. A., 1956, "Rational Choice and the Structure of the Environment," *Psychological Review*,
 858 vol. 63, no. 2, pp. 129–138.

859 12. Mistree, F., Hughes, O. F., and Bras, B., 1993, "Compromise Decision Support Problem And The
 860 Adaptive Linear Programming Algorithm," *Structural Optimization: Status And Promise*, (1993), pp.
 861 251-290.

862 13. Sharma, G., Allen, J. K., and Mistree, F., 2023, "Exploring Robust Decisions in the Design of Coupled
 863 Engineered Systems," *Journal of Mechanical Design*, pp. 1-35.

864 14. Chen, W., Simpson, T., Allen, J., and Mistree, F., 1999, "Satisfying Ranged Sets of Design
 865 Requirements using Design Capability Indices as Metrics," *Engineering Optimization*, vol.31, pp. 615-
 866 639.

867 15. Choi, H. J., Austin, R., Allen, J. K., McDowell, D. L., Mistree, F., and Benson, D. J., 2005, "An
 868 Approach for Robust Design of Reactive Power Metal Mixtures Based on Non-deterministic Micro-
 869 scale Shock Simulation," *Journal of Computer-Aided Materials Design*, vol.12, no.1, pp. 57-85.

870 16. Adams, B., Kalidindi, S., and Fullwood, D. T., 2013, "Microstructure Sensitive Design for Performance
 871 Optimization," *Butterworth-Heinemann*, Waltham, MA.

872 17. Kalidindi, S. R., Niezgoda, S. R., Landi, G., Vachhani, S. J., and Fast, T., 2010, "A Novel Framework
 873 for Building Materials Knowledge Systems," *Computers, Materials & Continua*, vol. 17, no. 2, pp. 103-
 874 126.

875 18. Kalidindi, S. R., Niezgoda, S. R., and Salem, A. A., 2011, "Microstructure informatics using higher-
 876 order statistics and efficient data-mining protocols," *JOM: The Journal of the Minerals, Metals &*
 877 *Materials Society*, vol. 63, no. 4, pp. 34-41.

878 19. Ghosh, S., Anantha Padmanabha, G., Peng, C., Andreoli, V., Atkinson, S., Pandita, P., Vandeputte, T.,
 879 Zabaras, N., and Wang, L., 2021, "Inverse Aerodynamic Design of Gas Turbine Blades Using
 880 Probabilistic Machine Learning," *Journal of Mechanical Design*, vol. 144, no. 2, p. 021706.

881 20. Sui, F., Guo, R., Zhang, Z., Gu, G. X., and Lin, L., 2021, "Deep Reinforcement Learning for Digital
 882 Materials Design," *ACS Materials Letters*, vol. 3, no. 10, pp. 1433-1439.

883 21. Chen, C. T., and Gu, G. X., 2020, "Generative Deep Neural Networks for Inverse Materials Design
 884 Using Backpropagation and Active Learning," *Advanced Science*, vol. 7, p. 1902607.

885 22. Kumar, S., Tan, S., Zheng, L., and Kochmann, D. M., 2020, "Inverse-Designed Spinodoid
 886 Metamaterials," *npj Computational Materials*, vol. 6, no. 1, p. 73.

887 23. Tsai, K.-M., and Luo, H.-J., 2017, "An Inverse Model for Injection Molding of Optical Lens using
 888 Artificial Neural Network Coupled with Genetic Algorithm," *Journal of Intelligent Manufacturing*, vol.
 889 28, no. 2, pp. 473-487.

890 24. Qian, C., Tan, R. K., and Ye, W., 2022, "Design of Architected Composite Materials with an Efficient,
 891 Adaptive Artificial Neural Network-Based Generative Design Method," *Acta Materialia*, vol. 225, p.
 892 117548.

893 25. Martins, J. R. R. A., and Lambe, A. B., 2013, "Multidisciplinary Design Optimization: A Survey of
 894 Architectures," *AIAA Journal*, vol. 51, no. 9, pp. 2049-2075.

895 26. Wang, P., Bai, Y., Fu, C., and Lin, C., 2023, "Lightweight design of an electric bus body structure with
 896 analytical target cascading," *Frontiers of Mechanical Engineering*, vol. 18, no.1, p. 2.

897 27. Kroo, I., Altus, S., Braun, R., Gage, P., and Sobieski, I., 1994, "Multidisciplinary Optimization Methods
 898 for Aircraft Preliminary Design," *Proceedings of the 5th Symposium on Multidisciplinary Analysis and*
 899 *Optimization*, September 1994, Panama City Beach, FL, U.S.A, Paper No. AIAA-1994-4325.

900 28. Sobiesczanski-Sobieski, J., and Kodiyalam, S., 2001, "BLISS/S: A New Method for Two-Level
 901 Structural Optimization," *Structural and Multidisciplinary Optimization*, vol. 21, no. 1, pp. 1-13.

902 29. Sobiesczanski-Sobieski, J., Agte, J., and Robert Sandusky, J., 1998, "Bi-level Integrated System
 903 Synthesis (BLISS)," *7th AIAA/USAF/NASA/ISSMO Symposium on Multidisciplinary Analysis and*
 904 *Optimization*, St. Louis, M.O., U.S.A, Paper No. AIAA-98-4916, pp. 1543-1557.

905 30. Flores Ituarte, I., Panicker, S., Nagarajan, H. P. N., Coatanea, E., and Rosen, D. W., 2022,
 906 "Optimisation-Driven Design to Explore and Exploit the Process–Structure–Property–Performance
 907 Linkages in Digital Manufacturing," *Journal of Intelligent Manufacturing*, vol. 34, pp. 219–241.

908 31. Shahani, D. W., and Seepersad, C. C., 2012, "Bayesian Network Classifiers for Set-Based Collaborative
909 Design," *Journal of Mechanical Design*, vol. 134, no. 7, p. 071001.
910 32. Baby, M., Nellippallil, A. B., 2023, "An Information-Decision Framework for the Multilevel Co-Design
911 of Products, Materials, and Manufacturing Processes " *Advanced Engineering Informatics* (under
912 review)
913 33. Thole, S. P., and Ramu, P., 2020, "Design Space Exploration and Optimization Using Self-Organizing
914 Maps," *Structural and Multidisciplinary Optimization*, vol. 62, no. 3, pp. 1071-1088.
915 34. McDowell, D. L., Panchal, J. H., Choi, H.-J., Seepersad, C. C., Allen, J. K., and Mistree, F., 2010,
916 "Chapter 8 - Integrated Design of Materials and Products—Robust Design Methods for Multilevel
917 Systems," *Integrated Design of Multiscale, Multifunctional Materials and Products*, Butterworth-
918 Heinemann, Boston, pp. 179-240.
919 35. Richardson, T., Kannan, H., Bloebaum, C., and Winer, E., 2014, "Incorporating Value-Driven Design
920 into the Visualization of Design Spaces Using Contextual Self-Organizing Maps: A Case Study of
921 Satellite Design," *15th AIAA/ISSMO Multidisciplinary Analysis and Optimization Conference*, Atlanta,
922 Georgia, U.S.A, Paper No. AIAA 2014-2728.
923 36. Kohonen, T., and Somervuo, P., 1998, "Self-organizing Maps of Symbol Strings," *Neurocomputing*,
924 vol. 21, no. 1, pp. 19-30.
925 37. Vesanto, J., 1999, "SOM-based Data Visualization Methods," *Intelligent Data Analysis*, vol. 3, no.2,
926 pp. 111-126.
927 38. Sushil, R. R., Baby, M., Sharma, G., Balu Nellippallil, A., and Ramu, P., 2022, "Data Driven Integrated
928 Design Space Exploration Using iSOM," *ASME 2022 International Design Engineering Technical
929 Conferences and Computers and Information in Engineering Conference*, Paper. No. DETC2022-
930 89895.
931 39. Nagar, D., Pannerselvam, K., and Ramu, P., 2022, "A Novel Data-Driven Visualization of n-
932 Dimensional Feasible Region using interpretable Self-Organizing Maps (iSOM)," *Neural Networks*,
933 vol. 155, pp. 398-412.
934 40. Nagar, D., Ramu, P., and Deb, K., 2023, "Visualization and Analysis of Pareto-Optimal Fronts using
935 interpretable Self-Organizing Map (iSOM)," *Swarm and Evolutionary Computation*, vol. 76, p.
936 101202.
937 41. Yadav, D., Nagar, D., Ramu, P., and Deb, K., 2023, "Visualization-aided Multi-Criteria Decision-
938 Making using interpretable Self-Organizing Maps," *European Journal of Operational Research*, vol.
939 309, no. 3, pp. 1183-1200.
940 42. Gladman, T. M. I., and Pickering, F., 1972, "Some Aspects of the Structure-Property Relationships in
941 High-C Ferrite-Pearlite Steels," *Journal of the Iron and Steel Institute*, vol. 210, no. 12, pp. 916-930.
942 43. Hodgson, P., and Gibbs, R., 1992, "A Mathematical Model to Predict the Mechanical Properties of Hot
943 Rolled C-Mn and Microalloyed Steels," *ISIJ International*, vol. 32, no. 12, pp. 1329-1338.
944 44. Kuziak, R., Cheng, Y.-W., Glowacki, M., and Pietrzyk, M., 1997, "Modeling of the Microstructure and
945 Mechanical Properties of Steels during Thermomechanical Processing," *NIST Technical Note (USA)*,
946 vol. 1393, p. 72.
947 45. Yada, H., 1988, "Prediction of Microstructural Changes and Mechanical Properties in Hot Strip
948 Rolling," *Proceedings of the Metallurgical Society of the Canadian Institute of Mining and Metallurgy*,
949 Elsevier, pp. 105-119.

950 **APPENDIX A**

951 In Table A1, we present the empirical models that relate the steel microstructure and composition with
952 the steel rod properties. These models are employed in modeling the decision problem at Design Level 1, as
953 described in Block B of Section 4. The YS_{lower} , YS_{mean} , and YS_{upper} models depict the uncertainties in the YS
954 model, as described in Step A2, Block A of Section 4.

955 **TABLE A1: Empirical models for mechanical property goals at Design Level 1**

956 $(T_{mf} = 700^{\circ}C, p = 6\mu\text{m}, t_{carb} = 0.025\mu\text{m})$

Mechanical Property	Empirical Model	Source
$YS_{lower} [f_2(x)]$	$X_f(77.7 + 59.9[Mn] + 9.1(D_a \cdot 0.001)^{-0.5}) + 478[N]^{0.5} + 1200[P] + (1 - X_f)(145.5 + 3.5S_0^{-0.5})$	Kuziak and co-authors (1997) [44]
$YS_{mean} [f_o(x)]$	$63[Si] + 425[N]^{0.5} + X_f^{1/3}(35 + 58[Mn] + 17(0.001D_a)^{-0.5}) + (1 - X_f^{1/3})(179 + 3.9S_0^{-0.5})$	Gladman and co-authors (1972) [42]

YS_{upper} $f_1(x)$ 	$62.6 + 26.1[\text{Mn}] + 60.2[\text{Si}] + 759[\text{P}] + 212.9[\text{Cu}] + 3286[\text{N}] + 19.7(0.001D_a)^{-0.5}$	Hodgson & Gibbs (1992) [43]
TS	$X_f(20 + 2440[\text{N}]^{0.5} + 18.5(0.001*D_a)^{-0.5} + 750(1 - X_f) + 3(1 - X_f^{0.5}) S_0^{-0.5} + 92.5*[\text{Si}])$	Kuziac and co-authors (1997) [44]
HV	$X_f(361 - 0.357T_{mf} + 50[\text{Si}]) + 175(1 - X_f)$	Yada (1988) [45]

958

959

In Table A2, we present the empirical models that relate the steel microstructure and composition before cooling and the cooling processing parameters with the steel microstructure at the end of the cooling process. These models are employed in modeling the decision problem at Design Level 2, as described in Block B of Section 4.

960

961

962

963

TABLE A2: Empirical models for steel microstructure characteristics at the end of cooling at Design Level 2

Microstructure characteristics	Empirical Models	Source
D_a	$(1 - 0.45\varepsilon_f^{0.5}) * \{(-0.4 + 6.37*C_{eq}) + (24.2 - 59*C_{eq}) CR^{-0.5} + 22*(1 - \exp(-0.015*d_f))\}$	Hodgson & Gibbs (1992) [43]
S₀	$0.1307 + 1.027[\text{C}] - 1.993[\text{C}]^2 - 0.1108[\text{Mn}] + 0.0305*CR^{-0.52}$	Kuziac and co-authors (1997) [44]
X_{f eq}	$1 - ([\text{C}] / (0.789 - 0.1671[\text{Mn}] + (0.1607[\text{Mn}]^2) - (0.0448[\text{Mn}]^3)))$	Kuziac and co-authors (1997) [44]
X_f	$X_{f eq} - 5.48(1 - \exp(-0.0106CR)) - (0.723*(1 - \exp(-0.0009d_f)))$	Kuziac and co-authors (1997) [44]
C_{eq}	$([\text{C}] + [\text{Mn}])/6$	Hodgson & Gibbs (1992) [43]

964